

# VII CHAPTER : COMPLEX METAL-HYDRIDES

VII.1	Introduction	2
VII.2	Complex Transition metal-hydrides	3
	VII.2.1 Structures and properties	3
	VII.2.2 Systematic trends and predictive concepts	9
VII.3	$Mg_2NiH_4$	13
VII.4	Square planar cluster	18
VII.5	Octahedral cluster	24
VII.6	Alanes	27
VII.7	References	30

## VII.1 INTRODUCTION

Until now we have dealt with metal-hydride systems that act to some extent as a sponge. The simplest case was  $\text{PdH}_x$ : the metal Pd absorbs hydrogen up to  $x=1$  without structural changes except for a swelling by approximately 20%. Slightly more complicated are the group V metal-hydrides. In  $\text{VH}_x$ ,  $\text{NbH}_x$  and  $\text{TaH}_x$  there are some structural changes and ordering phenomena but they can still be described as genuine interstitial alloys. Here too the main effect is a volume swelling of the order of 20% and hydrogen occupies the largest interstitial sites. For  $\text{LaH}_x$  the situation gets somewhat more complicated. At low concentration the structure is HCP, while for  $2 < x < 3$  it is FCC. In the HCP phase there is a large volume expansion and between the dihydride and the trihydride phase a small contraction. There is also strong evidence that hydrogen in  $\text{LaH}_x$  and  $\text{YH}_x$  is negatively charged ( $\text{H}^-$  ion). In  $\text{YH}_x$  there is an extra structural complication in the trihydride phase. The hydrogen atoms do not occupy the obvious octahedral interstitial sites of the Y host lattice but have moved towards the Y planes where they occupy smaller interstitial sites. This, by the way, is also what happens in  $\text{LaH}_x$ : first hydrogen enters the small tetrahedral sites (up to  $x=2$ ) and then starts to occupy the larger octahedral sites of the  $\text{CaF}_2$  structure.

In the present Chapter we consider an even more complicated family of metal hydrides: the so-called "Complex hydrides". One distinguishes complex hydrides of transition metals and complex hydridoborates and hydridoaluminates usually called „boranates“ (e.g.  $\text{NaBH}_4$ ) and „alanates“ (e.g.  $\text{LiAlH}_4$ ). Both families provide new opportunities for hydrogen storage (see Table VII.1). For example, the hydrogen-to-metal ratio of transition metal hydrides reaches values up to  $\text{H/M} = 4.5$  (for  $\text{BaReH}_9$ ) which is larger than the hydrogen-to-carbon ratios of hydrocarbons (methane:  $\text{H/C} = 4$ ); their hydrogen volume efficiencies exceed that of liquid hydrogen by a factor of up to two (for  $\text{Mg}_2\text{FeH}_6$ ), their weight efficiencies exceed 5% (for  $\text{Mg}_3\text{MnH}_7$ ), and their hydrogen dissociation temperatures under 1 bar hydrogen pressure range from about  $100^\circ\text{C}$  (for  $\text{NaKReH}_9$ ) to  $400^\circ\text{C}$  (for  $\text{CaMgNiH}_4$ ). The alanates and borates are, in principle, even better for hydrogen storage.

Table VII.1: Molecular weight and weight percentage of hydrogen in some complex alkaline and alkaline-earth hydrides.

		M	H / M
		[g mol <sup>-1</sup> ]	[wt%]
Lithiumboro-hydride	<b>LiBH<sub>4</sub></b>	21.784	18.4
Sodiumboro-hydride	<b>NaBH<sub>4</sub></b>	37.83	10.6
Potassiumboro-hydride	<b>KBH<sub>4</sub></b>	53.94	7.4
Lithiumaluminum-hydride	<b>LiAlH<sub>4</sub></b>	37.95	9.5
Sodiumaluminum-hydride	<b>NaAlH<sub>4</sub></b>	54.0	7.4
Sodiumaluminum-hydride	<b>Na<sub>3</sub>AlH<sub>6</sub></b>	102.0	5.9
Sodiumlithiumaluminum-hydride	<b>Na<sub>2</sub>LiAlH<sub>6</sub></b>	85.9	7.0
Magnesiumnickel-hydride	<b>Mg<sub>2</sub>NiH<sub>4</sub></b>	111.3	3.6
Magnesiumiron-hydride	<b>Mg<sub>2</sub>FeH<sub>6</sub></b>	110.5	5.4
Magnesiummanganese-hydride	<b>Mg<sub>3</sub>MnH<sub>7</sub></b>	134.9	5.2

The complex metal-hydrides are also fascinating materials for fundamental research since now the hydrogen is bound to the transition metal (Ni, Fe, ...) or a simple metal (Al,...) or B to form a charged complex. Their crystal chemistry is extremely rich and many transition metal hydrido-complexes often conform to the so-called 18-electron rule.

## VII.2 COMPLEX TRANSITION METAL-HYDRIDES

Complex transition metal hydrides constitute a relatively recent and somewhat exotic class of solid state compounds. The historically first member and text book example is  $K_2ReH_9$ . It was reported in 1964 and found to contain tricapped trigonal prismatic  $[Re(VII)H_9]^{2-}$  complex anions in which rhenium is fully oxidised. The second member,  $Sr_2RuH_6$ , was reported in the seventies and found to contain an octahedral  $[Ru(II)H_6]^{4-}$  complex. Wider interest in these compounds started only in the eighties after the discovery of typically metallic transition metal hydrides, such as  $LaNi_5H_6$  and  $FeTiH_2$  (see Chapter IX), which have reached commercial maturity<sup>1</sup> for reversible hydrogen storage in batteries for portable electronics (mobile phones, laptops,...). One of these compounds, however, was non-metallic ( $Mg_2NiH_4$ ) and showed a nearly fixed hydrogen content. This compound was classified as a complex transition metal hydride after its structure had been fully characterised and found to contain discrete tetrahedral  $[Ni(0)H_4]^{4-}$  complexes. [Note, however, that recent theoretical work by Garcia et al suggest that the arrangement of the four hydrogen atoms around Ni form a tetrahedrally distorted square]. This triggered an intense activity in the field and led to the discovery of many other homoleptic hydrido complexes, such as octahedral  $[FeH_6]^{4-}$ , square-pyramidal  $[CoH_5]^{4-}$ , square-planar  $[PtH_4]^{2-}$ , and linear  $[PdH_2]^{2-}$ . Most of that work has been performed in the groups of Yvon<sup>2</sup> in Geneva, Bronger<sup>3</sup> in Aachen and Noreus<sup>4</sup> in Stockholm.

In 1994 some 25 complex ternary hydride structure types were known and have been reviewed<sup>2</sup>. Since then, their number has increased steadily and by now over 40 structure types representing more than 70 ternary and quaternary metal hydrides are known. Most of them have hydrogen volume storage capacities that exceed that of liquid hydrogen, but are either too heavy, too expensive, or thermally too stable for reversible hydrogen storage applications at room temperature. The aim of today's research is to find lighter and cheaper hydrides which decompose at or near ambient conditions, to develop new predictive concepts, to find new synthetic routes, and to understand the factors that govern hydride formation, hydrogen contents and thermal stability. This is one of the most important field of research of the Dutch NWO program "Sustainable Hydrogen".

The presently known complex metal hydrides are based on late transition elements (group 7-10, including Cu and Zn), and monovalent or divalent metals (M) belonging to the alkali or alkaline-earth and lanthanide series, respectively. Most are true ternary (or quaternary) compounds in the sense that they do not derive from stable intermetallic parent compounds. They can only be synthesised as polycrystalline materials by solid state reactions from the elements and/or binary hydrides (MH or  $MH_2$ ) at temperatures typically between 300°C and 500°C, and hydrogen pressures between 1 and 100 bar. Some, however, can only be prepared by solution methods, reaction in a high temperature anvil pressure cell, mechanical alloying, or the use of a LiH flux to increase the yield (see examples below).

### VII.2.1 STRUCTURES AND PROPERTIES

The most striking structural feature of the transition metal hydrido-complexes is that they contain complexes  $[TH_x]^{n-}$  where x varies between 2 and 9, and n adopts values from 2 to 5. These

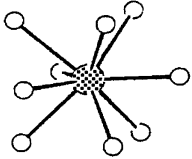
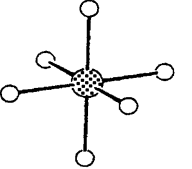
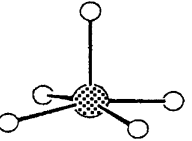
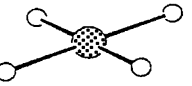
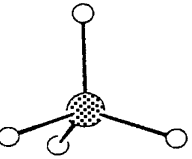
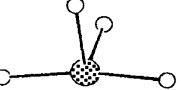
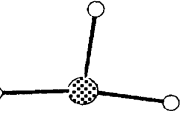
	complex	electron configuration	electrons per complex
	[ReH <sub>9</sub> ] <sup>2-</sup> [TcH <sub>9</sub> ] <sup>2-</sup>	(d <sup>0</sup> )-d <sup>5</sup> sp <sup>3</sup> (d <sup>0</sup> )-d <sup>5</sup> sp <sup>3</sup>	18 18
	[MnH <sub>6</sub> ] <sup>5-</sup> [ReH <sub>6</sub> ] <sup>5-</sup> [FeH <sub>6</sub> ] <sup>4-</sup> [RuH <sub>6</sub> ] <sup>4-</sup> [OsH <sub>6</sub> ] <sup>4-</sup> [RhH <sub>6</sub> ] <sup>3-</sup> [IrH <sub>6</sub> ] <sup>3-</sup> [PtH <sub>6</sub> ] <sup>2-</sup>	(d <sup>6</sup> )-d <sup>2</sup> sp <sup>3</sup> (d <sup>6</sup> )-d <sup>2</sup> sp <sup>3</sup>	18 18 18 18 18 18 18 18
	[RuH <sub>5</sub> ] <sub>av</sub> <sup>5-</sup> [CoH <sub>5</sub> ] <sup>4-</sup> [IrH <sub>5</sub> ] <sub>av</sub> <sup>4-</sup>	(d <sup>8</sup> )-dsp <sup>3</sup> (d <sup>8</sup> )-dsp <sup>3</sup> (d <sup>8</sup> )-dsp <sup>3</sup>	18 18 18
	[RhH <sub>4</sub> ] <sup>3-</sup> [PdH <sub>4</sub> ] <sup>2-</sup> [PtH <sub>4</sub> ] <sup>2-</sup>	(d <sup>8</sup> )-dsp <sup>2</sup> (d <sup>8</sup> )-dsp <sup>2</sup> (d <sup>8</sup> )-dsp <sup>2</sup>	16 16 16
	[MnH <sub>4</sub> ] <sup>2-</sup> [NiH <sub>4</sub> ] <sup>4-</sup> [CuH <sub>4</sub> ] <sup>3-</sup> [ZnH <sub>4</sub> ] <sup>2-</sup>	(d <sup>5</sup> )-sp <sup>3</sup> (d <sup>10</sup> )-sp <sup>3</sup> (d <sup>10</sup> )-sp <sup>3</sup> (d <sup>10</sup> )-sp <sup>3</sup>	13 18 18 18
	[CoH <sub>4</sub> ] <sub>av</sub> <sup>5-</sup> [RuH <sub>4</sub> ] <sup>4-</sup>	(d <sup>8</sup> )-dsp <sup>3</sup> (d <sup>8</sup> )-dsp <sup>2</sup>	18 16*)
	[RuH <sub>3</sub> ] <sup>6-</sup> [PdH <sub>3</sub> ] <sub>av</sub> <sup>3-</sup>	? (d <sup>10</sup> )-sp <sup>2</sup>	17*) 16
	[PdH <sub>2</sub> ] <sup>2-</sup>	(d <sup>10</sup> )-sp	14

Fig. VII.1: The various complexes found in complex metal-hydrides. (from Yvon<sup>5</sup>). Indicated are the ligand geometries, likely electron configurations and electron counts for transition metal hydrido complexes ; *av* : average due to disorder ; \*) possible metal-metal bonds (see text).

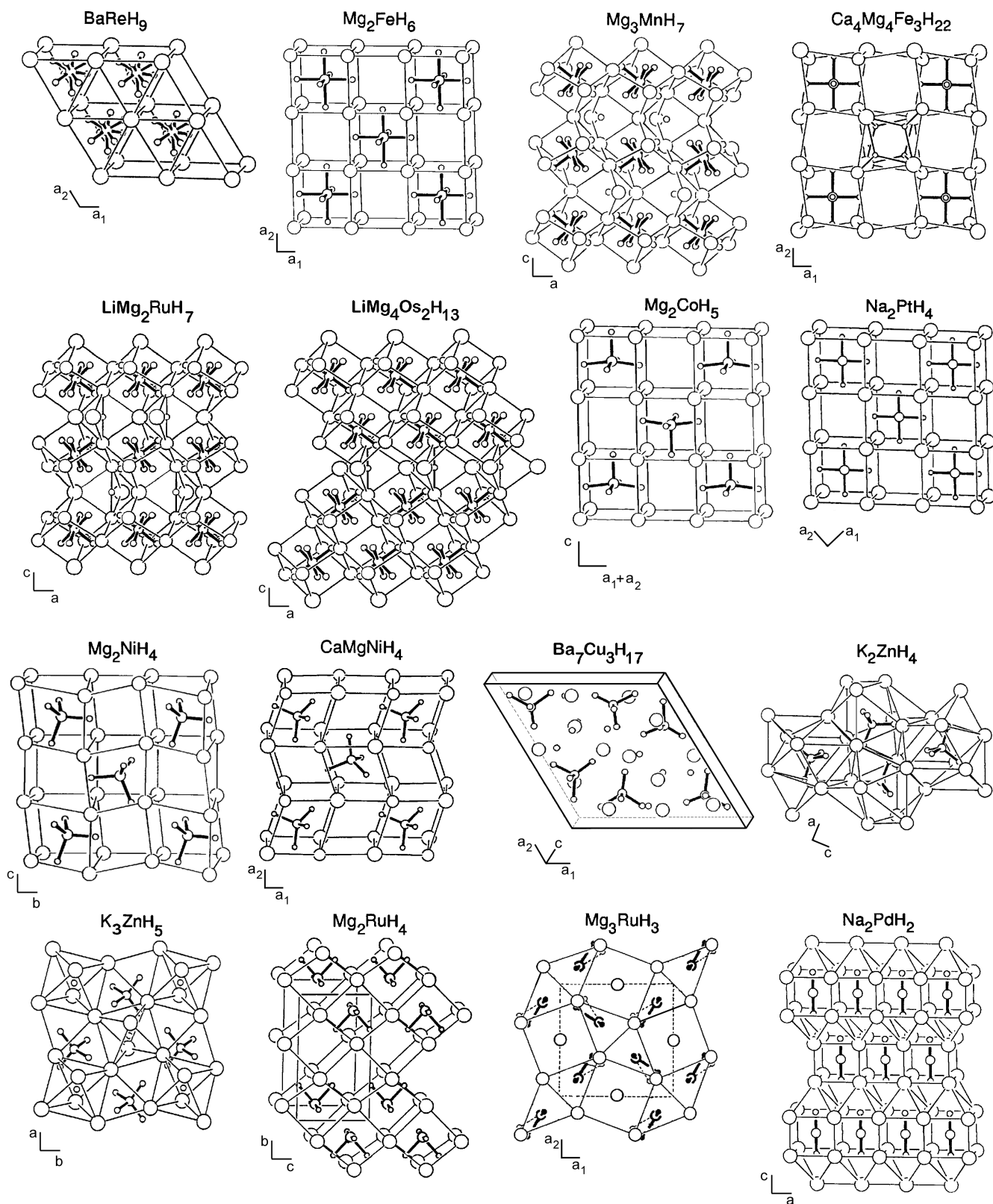


Fig. VII.2: The various structures of the complex transition metal hydrides (Yvon) Fig. 2: crystal structures of solid state complex transition metal hydrides;  $\text{TH}_x$  complexes are drawn by heavy lines, disordered ligands by dashed lines, M-M contacts by single lines, M atoms as large circles, and H atoms as small isolated circles.

complexes exhibit the various ligand geometries and electronic configurations shown in Fig. VII.1. There is a striking tendency to form complexes with 18 electrons (this is the basis for the so-called 18 electron rule) which suggests that each complex behaves like a pseudo-atom with a closed electronic shell.

Some structures also contain hydrogen anions  $\text{H}^-$  bonded to non-transition metals only. Together, these two hydride species (complexes and  $\text{H}^-$  anions) lead to a great variety of crystal structures and properties. In the following, they will be discussed by referring to typical representatives of the most common ligand geometries. The various crystal structures are represented in Fig. VII.2.

We give now extensive structural and physical information for typical transition metal complex hydrides for the reader actively involved in research on these materials. Of these data, which have graciously been made available by Klaus Yvon, students should at least remember that the smallest H-H distances for all the compounds is rather constant (between 1.94 and 2.66 Å) which is close to twice the radius of the  $\text{H}^-$  ion calculated in the preceding Chapter. Furthermore, in all complex hydrides the smallest distance between transition metal atoms is always much larger than in the parent metal. This leads to very flat d-bands in these materials.

### ***Tricapped trigonal prismatic complexes***

$\text{BaReH}_9$  : was prepared by a solution method<sup>6</sup> the hexagonal structure contains  $[\text{ReH}_9]^{2-}$  18-electron complexes whose H positions were inferred from infra-red and NMR data. It has the highest hydrogen-to-metal ratio known (H/M=4.5), a good hydrogen volume efficiency (134 gH<sub>2</sub>/liter) and a low dissociation temperature (<100°C at 1 bar), but is too heavy (weight efficiency 2.7%) and too expensive for large scale storage applications. No analogues (except for technetium) are known.  $[\text{ReH}_9]^{2-}$  complexes also occur in  $\text{K}_2\text{ReH}_9$  and  $\text{NaKReH}_9$  which<sup>7</sup> desorb hydrogen below 100°C.

### ***Octahedral complexes***

$\text{Mg}_2\text{FeH}_6$  : originally prepared as a green powder by sintering at 500°C and 20-120 bar hydrogen pressure, it can also be obtained under milder conditions by mechanical alloying. The cubic  $\text{K}_2\text{PtCl}_6$  type structure contains octahedral  $[\text{FeH}_6]^{4-}$  18-electron complexes which are surrounded by  $\text{Mg}^{2+}$  in a cubic configuration. It has a very high hydrogen volume storage efficiency (150 g/liter), a good weight efficiency (5.4 wt.%), and is cheap to fabricate, but it is too stable for reversible storage applications at room temperature (**desorption** enthalpy  $\Delta\text{H}=49$  kJ/mole H, decomposition temperature at 1 bar 320°C). It is non-metallic and Mössbauer spectra are consistent with low-spin Fe(II). Analogues exist for  $\text{M}_2\text{TH}_6$  (M=Mg,Ca,Sr,Yb,Eu; T=Fe,Ru,Os) and  $\text{M}_2\text{PtH}_6$  (M=Na,K [3]) ; most are moisture sensitive and some are pyrophoric ( $\text{Mg}_2\text{OsH}_6$ ); due to matrix effects the Fe-H bond distances increase from 1.56 Å to 1.62 Å if Mg is substituted by Ca;  $(\text{H-H})_{\text{min}}=2.20$  Å ; theoretical band gaps range from 1.3 eV ( $\text{Sr}_2\text{FeH}_6$ ) to 4.0 eV ( $\text{Mg}_2\text{OsH}_6$ ); most compounds are diamagnetic, except  $\text{Eu}_2\text{RuH}_6$  (red) which is paramagnetic and orders magnetically below  $T_C=49\text{K}$  ; octahedral  $[\text{FeH}_6]^{4-}$  complexes also occur in quaternary<sup>8</sup>  $\text{SrMg}_2\text{FeH}_8$  .

$\text{Mg}_3\text{MnH}_7$  : recently prepared as a reddish powder by application of high pressure (20 kbar) in a multi-anvil cell<sup>9</sup>. The hexagonal structure contains octahedral  $[\text{Mn(I)H}_6]^{5-}$  18-electron complexes (Mn-H=1.63 Å); an additional hydride anion is co-ordinated by a  $\text{Mg}^{2+}$  trigonal bipyramid (H-

Mg=1.87 Å (2x), 2.71 Å (3x); (H-H)<sub>min</sub>=2.29 Å). The compound has promising hydrogen storage properties: 5.2 wt.%, 118.5 g H<sub>2</sub>/liter, decomposition at 1 bar starts at 240°C. An isostructural rhenium analogue exists.

Ca<sub>4</sub>Mg<sub>4</sub>Fe<sub>3</sub>H<sub>22</sub>: typical example for a quaternary hydride that derives from a ternary hydride (Mg<sub>2</sub>FeH<sub>6</sub>) by ordered cation substitution. In the cubic structure every fourth [FeH<sub>6</sub>]<sup>4-</sup> is replaced by four hydrogen anions which are tetrahedrally co-ordinated by M<sup>2+</sup>; Fe-H = 1.56-1.58 Å, M-H=1.81 Å (Mg), 2.39 Å (Ca), (H-H)<sub>min</sub>=2.22 Å; is thermally more stable (ΔH=61 kJ/mole H) than Mg<sub>2</sub>FeH<sub>6</sub>; decomposes in two steps *via* Ca<sub>2</sub>FeH<sub>6</sub>; brownish translucent single crystals can be grown in a LiH flux.

LiMg<sub>2</sub>RuH<sub>7</sub>: typical example for an intergrowth structure obtained by reaction of Mg<sub>2</sub>RuH<sub>6</sub> with LiH; the hexagonal structure<sup>10</sup> shows Mg<sub>2</sub>RuH<sub>6</sub> like slabs made up by single layers of octahedral [RuH<sub>6</sub>]<sup>4-</sup> complexes which are intergrown with LiH sheets; Ru-H=1.70 Å; (H-H)<sub>min</sub>=2.46 Å; H<sup>-</sup> anions have a trigonal bipyramidal co-ordination by Li<sup>+</sup> and Mg<sup>2+</sup> (M-H=1.85 Å (2Mg), 2.71 Å (3Li)); isostructural analogue exists for osmium but not for iron.

LiMg<sub>4</sub>Os<sub>2</sub>H<sub>13</sub>: hexagonal intergrowth structure as above, except that the Mg<sub>2</sub>OsH<sub>6</sub> like slabs are made up by double layers of octahedral [OsH<sub>6</sub>]<sup>4-</sup> complexes<sup>11</sup>; Os-H=1.70 Å; (H-H)<sub>min</sub>=2.31 Å; evidence for isostructural analogue exists for ruthenium, but not for iron.

### **Square pyramidal complexes**

Mg<sub>2</sub>CoH<sub>5</sub>: tetragonal structure is similar to cubic Mg<sub>2</sub>FeH<sub>6</sub>, except that it contains square pyramidal [CoH<sub>5</sub>]<sup>4-</sup> 18-electron complexes (Co-H=1.52 Å (basal), 1.59 Å (apical)); (H-H)<sub>min</sub>=2.12 Å; transforms at 488 K into a disordered cubic high-temperature (HT) modification; presumably nonmetallic; theoretical band gap 1.9 eV, weakly paramagnetic (possibly diamagnetic); ΔH=43 kJ/moleH; evidence for isostructural iridium analogues M<sub>2</sub>IrH<sub>5</sub> (M=Mg,Ca,Sr) but not for rhodium analogue Mg<sub>2</sub>RhH<sub>5</sub>; square pyramidal hydride complexes presumably also occur in partially disordered Mg<sub>6</sub>Co<sub>2</sub>H<sub>11</sub>, Mg<sub>3</sub>RuH<sub>6</sub> and M<sub>4</sub>Mg<sub>4</sub>Co<sub>3</sub>H<sub>19</sub> (M=Ca,Yb)<sup>12</sup>

### **Square planar complexes**

Na<sub>2</sub>PtH<sub>4</sub>: tetragonal structure [3] contains [Pt(II)H<sub>4</sub>]<sup>2-</sup> 16-electron complexes (Pt-H=1.64 Å) surrounded by Na<sup>+</sup> in a cubic configuration; (H-H)<sub>min</sub>=2.32 Å; transforms at about 300°C into a disordered cubic HT modification; red-violet, non-metallic, diamagnetic powder; theoretical band gap 1.2 eV; Pd, Cs and K analogues exist; square planar complexes also occur in Li<sub>3</sub>RhH<sub>4</sub>, K<sub>2</sub>PtH<sub>4</sub>, K<sub>3</sub>PtH<sub>5</sub> and Ba<sub>2</sub>PtH<sub>6</sub>; those in K<sub>2</sub>PtH<sub>4</sub> undergo in-plane rotational motions as shown by NMR data.

### **Tetrahedral complexes**

Mg<sub>2</sub>NiH<sub>4</sub>: monoclinic structure contains tetrahedral [NiH<sub>4</sub>]<sup>4-</sup> 18-electron complexes which are surrounded by Mg<sup>2+</sup> in a strongly distorted cubic configuration; sp<sup>3</sup> bonded Ni(0) has bond lengths Ni-H=1.54-1.57 Å and bond angles H-Ni-H=103°-119°; (H-H)<sub>min</sub>=2.43 Å; dark-red (fully hydrided) or brownish (partially hydrided) powder; diamagnetic and non-metallic; can be obtained by hydrogenation of the binary alloy Mg<sub>2</sub>Ni, and by mechanical alloying; microtwinning parallel to *bc* plane is consistent with a structural transformation at ~230°C into a disordered cubic HT modification; theoretical band gap 1.8 eV; has a good hydrogen storage efficiency: 3.6 wt.%, 98 g/liter; thermal stability (ΔH=32 kJ/mole H, desorption temperature

280°C at 1 bar) is sufficiently low for reversible hydrogen storage applications in automobiles ; no structural analogues are known.

$\text{CaMgNiH}_4$  : ordered quaternary derivative of  $\text{Mg}_2\text{NiH}_4$ ; the cubic structure contains a tetrahedral  $[\text{Ni}(0)\text{H}_4]^{4-}$  18-electron complex which is surrounded by a strongly distorted  $\text{M}^{2+}$  cube; Ni-H=1.60 Å, M-H= 2.08 Å (Mg), 2.45 Å (Ca); (H-H)<sub>min</sub>=2.59 Å ; greenish powder ; translucent single crystals of yellow brownish colour can be obtained in a LiH flux; thermal stability ( $\Delta\text{H}=64$  kJ/mole H) is twice that of  $\text{Mg}_2\text{NiH}_4$ ; isostructural Sr and Yb analogues exist<sup>13</sup>.

$\text{Ba}_7\text{Cu}_3\text{H}_{17}$  : first structurally characterised hydrido Cu complex [13]; the trigonal structure contains tetrahedral  $[\text{CuH}_4]^{3-}$  18-electron complexes (Cu-H=1.64 -1.78 Å) and three types of tetrahedrally co-ordinated  $\text{H}^-$  anions (Ba-H=2.50-2.92 Å) ; Cu(I) is presumably  $sp^3$  hybridized similar to Ni(0) in  $\text{Mg}_2\text{NiH}_4$  and Zn(II) in  $\text{K}_2\text{ZnH}_4$  ; conspicuously short (H-H)<sub>min</sub>=1.94(4) Å ; prepared by hydrogenation of binary alloy at room temperature ; no analogues are known.

$\text{K}_2\text{ZnH}_4$  and  $\text{K}_3\text{ZnH}_5$  : first structurally characterised hydrido Zn complexes<sup>14</sup> ; the orthorhombic and tetragonal structures, respectively, contain tetrahedral  $[\text{Zn}(\text{II})\text{H}_4]^{2-}$  complexes (Zn-H=1.63-1.67 Å);  $\text{K}_3\text{ZnH}_5$  also contains hydrogen anions (H-K=2.77 - 2.79 Å); (H-H)<sub>min</sub>=2.66 Å ; prepared by solid state reaction and solution methods ; decompose *via* binary hydrides ; Zn-H bond lengths in Rb and Cs analogues increase to 1.67-1.70 Å [14b] due to matrix effects; magnetic Mn analogues  $\text{M}_3\text{MnH}_5$  (M=K,Rb,Cs) of pink colour have been recently synthesised at ~500°C under 3 kbar hydrogen gas pressure [15].

### **Saddle like complexes**

$\text{Mg}_2\text{RuH}_4$  : orthorhombic structure contains a saddle-like  $[\text{Ru}(0)\text{H}_4]^{4-}$  16-electron complex which derives from octahedral  $[\text{Ru}(\text{II})\text{H}_6]^{4-}$  by removal of two *cis* H ligands (Ru-H=1.67-1.68 Å; H-Ru-H=84.2°, 93.6°(*cis*), 170.3°(*trans*)) ; (H-H)<sub>min</sub>=2.23 Å ; complexes are surrounded by  $\text{Mg}^{2+}$  in a cubic configuration ; possible Ru-Ru interactions across neighbouring cube faces (Ru-Ru=3.24 Å) could lead to polyanionic  $[\text{Ru}_n\text{H}_{4n}]^{4n-}$  zig-zag chains running along *c*; reddish-brown to dark-red colour ; magnetic measurements consistent with  $d^8$  low-spin configuration; no Fe analogue is known; saddle like complexes presumably also occur in partially disordered  $\text{Mg}_6\text{Co}_2\text{H}_{11}$  ( $[\text{CoH}_4]^{5-}$ ).

### **T-shaped complexes**

$\text{Mg}_3\text{RuH}_3$  : tetragonal structure contains orientationally disordered T-shaped  $\text{RuH}_3$  units (Ru-H=1.71 Å, (H-H)<sub>min</sub>=2.52 Å) which are possibly joined to dimers by a Ru-Ru bond (3.31 Å); T-shaped  $[\text{PdH}_3]^{3-}$  units presumably occur in partially disordered  $\text{LiSr}_2\text{PdH}_5$ ; triangular  $[\text{PdH}_3]^{3-}$  units occur in ordered  $\text{NaBaPdH}_3$  [4].

### **Linear complexes**

$\text{Na}_2\text{PdH}_2$  : tetragonal structure [3] contains linear  $[\text{Pd}(0)\text{H}_2]^{2-}$  14-electron complexes (Pd-H=1.68 Å) surrounded by  $\text{Na}^+$  in a bicapped cubic configuration; melts at 408°C without decomposing; metallic conductivity measured on single crystals ; electronic band structure calculations predict filled *d* bands and metallic properties in 2 dimensions (*ab* plane) ; linear complexes also occur in  $\text{K}_3\text{PdH}_3$ .

## VII.2.2 SYSTEMATIC TRENDS AND PREDICTIVE CONCEPTS

### **Structural features**

**Hydrogen, a very flexible ligand** : the large variety of complex transition metal hydrides reflects the special bonding character of hydrogen which can occur in the same structure as a covalent bonded ligand and as an anion. Its small atomic size and high-field ligand character favours 18-electron compounds (about 70 representatives with group 7-10 elements including Cu and Zn). Compounds with 16 electrons (over a dozen representatives with Rh, Pd and Pt), or 14 electrons (half a dozen representatives with Pd and Pt) are less numerous. On the other hand, the relative softness of hydrogen as a ligand, and the relative stability of hydrogen as an anion, favour structural diversity. Illustrative examples are the quaternary hydrides  $\text{Ca}_4\text{Mg}_4\text{Fe}_3\text{H}_{22}$  and  $\text{Ca}_4\text{Mg}_4\text{Co}_3\text{H}_{19}$  which derive from ternary  $\text{Mg}_2\text{FeH}_6$  and  $\text{Mg}_2\text{CoH}_5$ , respectively, by the substitution of one fourth of the tetravalent transition metal complexes by four  $\text{H}^-$  anions each. Other examples are  $\text{Mg}_3\text{MnH}_7$ ,  $\text{Mg}_6\text{Co}_2\text{H}_{11}$  and  $\text{Mg}_3\text{RuH}_6$  which have similar metal atom substructures and yet are capable of accommodating rather different complex geometries and hydrogen anions.

**Hydrido complexes** : their occurrence across the transition metals series exhibits a clear trend (see Fig. VII.1) from high-coordination at the left (group 7 of the Periodic Table) to low-coordination at the right (group 10). The complexes are generally mononuclear and have terminal hydrogen ligands. Of particular interest are the members of the  $3d$  series, including Cu and Zn. They all form homoleptic hydrido complexes. Some adopt only one ligand geometry such as Ni, Cu and Zn (tetrahedral), while others adopt two geometries such as Mn (octahedral or tetrahedral) or Co (saddle like or square-pyramidal). The most prolific transition metal is Ru which adopts four geometries (saddle-like, T-shaped, square-pyramidal, octahedral), in contrast to its Fe congener which adopts only one (octahedral). Each hydride structure contains only one type of hydrido complex. Notable exceptions are  $\text{K}_2\text{ReH}_9$  (two crystallographically different  $[\text{ReH}_9]^{2-}$ ) and  $\text{Mg}_6\text{Co}_2\text{H}_{11}$  ( $[\text{CoH}_4]^{5-}$  and  $[\text{CoH}_5]^{4-}$ ). The only dinuclear complex known is  $[\text{Pt}_2\text{H}_9]^{5-}$  which has a bridging hydrogen and occurs in  $\text{Na}_5\text{Pt}_2\text{H}_9$  [16]. Hydrides containing heteronuclear complexes, or complexes formed by different transition metals have not yet been reported.

The hydrogen ligand geometries are consistent with those expected for transition metals in coordination compounds, *i.e.* they are octahedral such as in  $\text{Mo}(\text{CO})_6$  ( $d^6$ , 18 electrons), square planar such as in  $\text{Ni}(\text{CN})_4^{2-}$  ( $d^8$ , 16 electrons) and tetrahedral such as in  $\text{Ni}(\text{CO})_4$  ( $d^{10}$ , 18 electrons). The square pyramidal and saddle-like geometries are similar to those in  $\text{Co}(\text{CN})_5^{3-}$  ( $d^7$ , 17 electrons), and  $\text{Ru}(\text{CO})_4$  ( $\equiv\text{Ru}_3(\text{CO})_{12}$ ;  $d^8$ , 18 electrons, see below), respectively. Linear co-ordinations are also not uncommon for  $d^{10}$  systems. A trigonal bi-pyramidal hydrogen configuration similar to the ligand geometry in  $\text{Fe}(\text{CO})_5$  has not yet been reported. Some geometries represent only averages such as  $[\text{CoH}_4]_{\text{av}}^{5-}$ ,  $[\text{RuH}_5]_{\text{av}}^{5-}$ ,  $[\text{PdH}_3]_{\text{av}}^{3-}$  and  $[\text{IrH}_3]_{\text{av}}^{6-}$  because of disorder. The mobility of the hydrogen ligands (or complexes) at room temperature is generally high. Well characterised order-disorder transitions at or near room temperature occur in  $\text{Mg}_2\text{CoH}_5$ ,  $\text{Mg}_2\text{NiH}_4$ ,  $\text{K}_3\text{PdH}_3$ ,  $\text{Na}_2\text{PtH}_4$ ,  $\text{M}_3\text{PtH}_5$ , ( $\text{M}=\text{Rb}, \text{Cs}$ ), and  $\text{M}_2\text{PtH}_4$ , ( $\text{M}=\text{K}, \text{Rb}, \text{Cs}$ ).

**Hydrogen anions**: they occur in about half of the structures known and appear to be preferentially associated with 18 electron systems; the  $\text{H}^-$  anions are co-ordinated by  $\text{M}^+$  and/or  $\text{M}^{2+}$  cations in mostly tetrahedral ( $\text{SrMg}_2\text{FeH}_8$ ,  $\text{BaMg}_2\text{RuH}_8$ ,  $\text{Ca}_4\text{Mg}_4\text{Fe}_3\text{H}_{22}$ ) and linear (or trigonal bi-pyramidal) configurations ( $\text{LiMg}_2\text{RuH}_7$ ,  $\text{Mg}_3\text{MnH}_7$ ). Unlike the hydrogens in the complex, they are neither mobile nor disordered.

**Formal oxidation numbers:** the formal charges and electron counts can be rationalised in terms of limiting ionic formulas such as  $\text{Mg}_3\text{MnH}_7 = 3\text{Mg}^{2+} \cdot [\text{MnH}_6]^{5-} \cdot \text{H}^-$  (18 electrons),  $\text{Na}_2\text{PtH}_4 = 2\text{Na}^+ \cdot [\text{PtH}_4]^{2-}$  (16 electrons) and  $\text{Na}_2\text{PdH}_2 = 2\text{Na}^+ \cdot [\text{PdH}_2]^{2-}$  (14 electrons). The formal oxidation numbers of the transition elements range from *zero* (Ru, Ni, Pd), to *I* (Mn, Re, Co, Ir, Rh, Cu), *II* (Fe, Ru, Os, Pd, Pt, Zn), *III* (Ir, Rh), *IV* (Pt) and *VII* (Re). The situation in  $\text{Mg}_2\text{RuH}_4$  is particularly intriguing because its structure and electron count (formally 16 electrons/Ru) suggest Ru-Ru 2-electron bonds (two per Ru) which are linking the  $[\text{RuH}_4]^{4-}$  units to polymeric  $(\text{Ru}_n\text{H}_{4n})^{4n-}$  zig-zag chains. Thus each Ru could ‘see’ 18 electrons, although the metal-metal distances (Ru-Ru = 3.24 Å) are considerably longer than those in the metal-metal bonded trimer  $\text{Ru}_3(\text{CO})_{12}$  (Ru-Ru ~ 2.85 Å). Another intriguing case is  $\text{Mg}_3\text{RuH}_3$  (formally 17 electrons/Ru) which can be formulated as an 18-electron compound by postulating a Ru-Ru 2-electron bond connecting two  $[\text{RuH}_3]^{6-}$  monomers to a  $[\text{Ru}_2\text{H}_6]^{12-}$  dimer. The possibility of Ru-Ru bond formation in these compounds has been investigated theoretically [17].

**Metal-hydrogen bonds:** The T-H bond distances are in the range 1.50-1.60 Å for 3*d* metals, and 1.70-1.80 Å for 4*d* and 5*d* metals except for low co-ordinate Pd (1.60-1.70 Å) and Pt (1.58-1.67 Å). Due to matrix effects the bond lengths scale with the size of the M cations. The M-H bond distances of the complex hydrogen are generally longer than those in the corresponding binary metal hydrides. However, those of the anionic hydrogen - which is relatively low co-ordinate - are significantly shortened (Mg-H=1.81-1.87 Å, Ba-H=2.50 Å, K-H=2.77 Å) compared to the relatively high co-ordinate hydrogen in the corresponding binary metal hydrides  $\text{MgH}_2$  (1.95 Å),  $\text{BaH}_2$  (2.57 Å) and KH (2.85 Å).

**Hydrogen-hydrogen distances:** The H-H contacts usually exceed 2.1 Å, and thus indicate non-bonding (or repulsive) interactions. Contacts at less than 2.0 Å occur in  $\text{K}_2\text{ReH}_9$  and  $\text{Ba}_7\text{Cu}_3\text{H}_{17}$ . There is no evidence for hydrogen pairing, unlike for molecular transition metal hydride complexes in which di-hydrogen groups are known to occur<sup>15</sup>.

## Properties

**Electric conductivity, colour, magnetism, vibrational spectroscopy:** the quality and completeness of the published data generally depend on the availability of suitable single crystals ; most complex transition metal hydrides are polycrystalline and either experimentally found or theoretically predicted to be non-metallic ; many are coloured ; only few are metallic such as  $\text{Li}_2\text{PdH}_2$  and  $\text{Na}_2\text{PdH}_2$  ; many are diamagnetic, as expected from closed-shell configurations associated with low-spin  $d^6$  (octahedral),  $d^8$  (square-planar), and  $d^{10}$  (tetrahedral, linear) configurations; the compounds containing magnetic ions such as  $\text{Eu}^{2+}$  and  $\text{Mn}^{2+}$  show temperature dependent paramagnetism and order magnetically at low temperature. The known vibrational spectra (IR, inelastic neutron scattering) correlate with bonding properties, such as in the  $\text{K}_2\text{PtCl}_6$  type series, for which the T-H stretching frequencies increase in the sequence T=Fe,Ru,Os, and decrease as the M-H bond lengths increase. However, the picture concerning the electric, magnetic and spectroscopic properties is far from being complete and more data are needed.

**Hydrogen storage efficiencies :** The hydrogen-to-metal ratios reach values of up to H/M = 4.5 ( $\text{BaReH}_9$ ) and thus surpass the hydrogen-to-carbon ratios of hydrocarbons (methane : H/C=4) ; the hydrogen volume efficiencies reach 150g/liter ( $\text{Mg}_2\text{FeH}_6$ ) and thus exceed that of liquid hydrogen (71g/liter) by a factor of up to two. The weight efficiencies exceed 5% ( $\text{Mg}_2\text{FeH}_6$ ,  $\text{Mg}_3\text{MnH}_7$ ).

**Thermal stability**: the hydrides decompose in one or several steps with upper plateau temperatures at 1 bar hydrogen pressure in the range of about 100°C (NaKReH<sub>9</sub>) to 400°C (CaMgNiH<sub>4</sub>). The desorption enthalpies [note that in the rest of this lecture we gave the heat of formation or enthalpies of solution (formation) which have the opposite sign !] measured so far cover the range  $\Delta H=32 - 65$  kJ/mole H ; they are intermediate between those of typically metallic hydrides such as LaNi<sub>5</sub>H<sub>6</sub> ( $\Delta H=16$  kJ/mole H) and saline hydrides such as LiH ( $\Delta H=91$  kJ/mole H). Due to the scarcity of data, no satisfactory model exists which is capable of rationalising these enthalpies. Interactions between hydrogen and alkaline and/or alkaline earth elements appear to play a role, as can be seen from the two substitutional pairs Mg<sub>2</sub>NiH<sub>4</sub> ( $\Delta H=32$  kJ/mole H) - CaMgNiH<sub>4</sub> ( $\Delta H=65$  kJ/mole H) and Mg<sub>2</sub>FeH<sub>6</sub> ( $\Delta H=49$  kJ/mole H) - Ca<sub>4</sub>Mg<sub>4</sub>Fe<sub>3</sub>H<sub>22</sub> ( $\Delta H=61$  kJ/mole H), in which the stability increases strongly as one goes from the Mg based ternary to the Ca containing quaternary compound. This trend correlates with the thermal stability of binary CaH<sub>2</sub> ( $\Delta H=92$  kJ/mole H) which is much higher than that of MgH<sub>2</sub> ( $\Delta H=37$  kJ/mole H). Clearly, more data are necessary to put this type of correlation on a more quantitative basis.

### Criteria for hydride formation

**Magic electron numbers**: In contrast to metallic transition metal hydrides the composition of complex transition metal hydrides can be rationalised in terms of ‘magic’ electron counts. The Mg<sub>2</sub>FeH<sub>6</sub>-Mg<sub>2</sub>CoH<sub>5</sub>-Mg<sub>2</sub>NiH<sub>4</sub> series provides an illustrative example. Its hydrogen content decreases as the number of available *d* electrons increases, in accordance with the 18-electron rule. The usefulness of this approach is also apparent for 16- and 14-electron systems, and for hydride structures that contain both complex and anionic hydrogen such as Ca<sub>4</sub>Mg<sub>4</sub>Fe<sub>3</sub>H<sub>22</sub> and K<sub>3</sub>ZnH<sub>5</sub>. Their compositions clearly depend on the electron count of the complex and the valence of the metal cations. Thus the concept of ‘magic’ electron numbers has considerable predictive value.

**Structural intergrowth**: illustrative examples are the quaternary hydrides LiMg<sub>2</sub>OsH<sub>7</sub> (Li<sup>+</sup>H<sup>-</sup>.2Mg<sup>2+</sup>.[OsH<sub>6</sub>]<sup>4-</sup>) and LiMg<sub>4</sub>Os<sub>2</sub>H<sub>13</sub> (Li<sup>+</sup>H<sup>-</sup>.4Mg<sup>2+</sup>.2[OsH<sub>6</sub>]<sup>4-</sup>) which derive from ternary Mg<sub>2</sub>OsH<sub>6</sub> by intergrowth with LiH. These can be considered as the first members (n=1,2) of a structural series having the general composition LiMg<sub>2n</sub>Os<sub>n</sub>H<sub>6n+1</sub>. The existence of members with n>2 is likely but not yet demonstrated. The intergrowth concept also applies to trigonal SrMg<sub>2</sub>FeH<sub>8</sub> (Mg<sub>2</sub>FeH<sub>6</sub> intergrown with SrH<sub>2</sub>) and tetragonal BaMg<sub>2</sub>RuH<sub>8</sub> (Mg<sub>2</sub>RuH<sub>6</sub> intergrown with BaH<sub>2</sub>) [19] although their M<sup>2+</sup> substructures become somewhat distorted.

**Substitutional derivatives**: quaternary metal hydride structures which can be considered as ordered derivatives of ternary hydride structures are Ca<sub>4</sub>Mg<sub>4</sub>Fe<sub>3</sub>H<sub>22</sub>, Ca<sub>4</sub>Mg<sub>4</sub>Co<sub>3</sub>H<sub>19</sub> and CaMgNiH<sub>4</sub>. The concept of atomic substitution is useful but obviously limited by matrix effects. The absence of Fe analogues for the various Ru and Os members of the above LiH intergrowth series, for example, could be due to a size mismatch between the relatively small [FeH<sub>6</sub>]<sup>4-</sup> complexes and the Li cations. Similar effects could also be responsible for the apparent absence of ternary hydrides such as ‘MgMnH<sub>9</sub>’, a possible derivative of isoelectronic BaReH<sub>9</sub>.

**Competing phases**: the thermodynamics of the phase diagram are also important ; this can be seen from the Mg-Rh-H system in which the competing phases Mg<sub>2</sub>RhH<sub>x</sub> (x~1) and Mg<sub>2</sub>Rh presumably prevent the formation of the expected hydride phase ‘Mg<sub>2</sub>RhH<sub>5</sub>’. The absence of complex hydrides with early transition metals such as Sc, Ti, V, etc. could have similar reasons. In contrast to late transition metals the latter form stable binary hydrides and intermetallic compounds with M elements, and this could prevent the formation of complex hydrides.

***Influence of pressure*** : A decisive parameter for hydride formation is pressure. The synthesis of hydrides based on light transition elements usually requires higher hydrogen pressures than that based on heavier congeners. Examples are the Pd compounds  $M_2PdH_4$  and  $M_3PdH_5$  which form at 20 and 70 bar, respectively, in contrast to their Pt congeners, which form already at 1 bar. For a given transition metal an increase of hydrogen pressure usually allows to stabilise higher formal oxidation states. Examples are found for palladium in  $M_3Pd(0)H_3$  and  $M_2Pd(II)H_4$  which form at 1 bar and 20 bar, respectively, for platinum in  $K_2Pt(II)H_4$  and  $K_2Pt(IV)H_6$  which form at 1 bar and 1800 bar respectively, and for ruthenium in  $Mg_2Ru(0)H_4$  and  $Mg_2Ru(II)H_6$  which form at 20 bar and 90 bar, respectively. However, the inverse situation appears to prevail for manganese based  $Mg_3Mn(I)H_7$  which forms under a mechanical pressure of 20 kbar, while  $K_3Mn(II)H_5$  forms under a gas pressure of 3 kbar only. It is reasonable to expect that high pressure techniques, together with other synthetic routes such as solution methods and mechanical alloying, will give access to further members of this class of compounds.

### ***Summary***

Complex transition metal hydrides constitute a fascinating class of solid state compounds. They have a rich crystal chemistry which combines features of co-ordination compounds and saline hydrides. Their structures are built up by homoleptic transition metal complexes which have up to nine ligands, by hydrogen anions and by non-transition metal cations. Hydrogen acts as a strong and flexible ligand which is capable of oxidising heavy transition elements to oxidation numbers of up to IV (Pt) and even VII (Re). Spectroscopic, magnetic, and thermodynamic properties have been reported but need to be completed. Many compounds have excellent hydrogen storage efficiencies but are either thermally too stable or too expensive for applications at room temperature. The main object of future work is to find advanced materials that combine high storage efficiency, low thermal stability and low fabrication costs, and to understand better the factors which influence thermodynamic properties. Some useful concepts for search exist, such as 'magic' electron counts, structural intergrowth and ordered substitution, but they need to be refined by first principle calculations and further experimental data.

### VII.3 $\text{Mg}_2\text{NiH}_4$

To get more insight in the electronic structure of complex transition metal hydrides we consider now in detail  $\text{Mg}_2\text{NiH}_4$ . Among the metal hydrides based on intermetallic compounds that are attractive for hydrogen storage, the compound  $\text{Mg}_2\text{Ni}$  occupies a special position. It reacts readily with gaseous hydrogen to form the stable hydride  $\text{Mg}_2\text{NiH}_4$ . Around  $300^\circ\text{C}$  the plateau pressure is of the order of several bars (see Fig. VII.3 and Chapter IX). It is therefore considered as a very convenient material for high temperature hydrogen storage. The reaction occurs by precipitation of  $\text{Mg}_2\text{NiH}_4$  from the hexagonal intermetallic compound  $\text{Mg}_2\text{Ni}$  upon hydrogen absorption. Hexagonal  $\text{Mg}_2\text{Ni}$ , which has a rather complicated crystal structure, is able to dissolve only a small amount of hydrogen, namely up to  $\text{Mg}_2\text{NiH}_{0.3}$ . During further absorption of

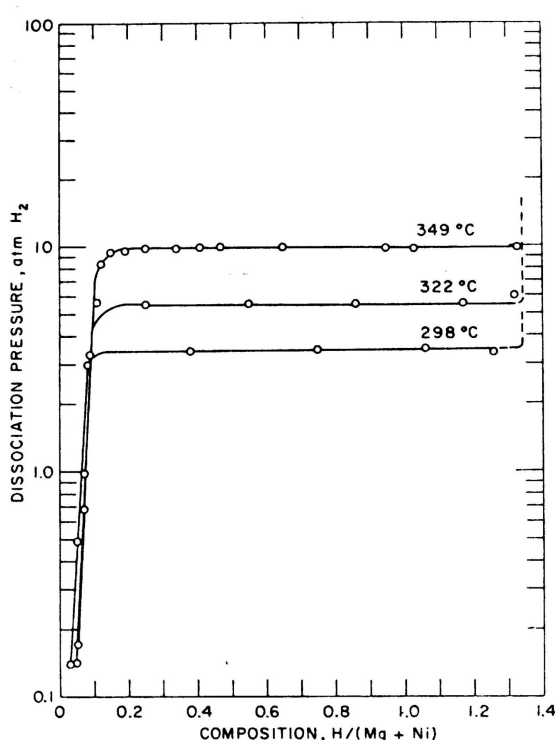


Fig. VII.3: P-c isotherms for hydrogen in  $\text{Mg}_2\text{Ni}$ .<sup>16</sup>

hydrogen a massive rearrangement of host metal atoms occurs while the molar volume increases by 32 %. The hydride  $\text{Mg}_2\text{NiH}_4$  is the only stable ternary compound observed in the Mg-Ni-H system. This compound shows a well-defined stoichiometry, essentially independent of temperature and hydrogen partial pressure. At 1 bar hydrogen pressure  $\text{Mg}_2\text{NiH}_4$  exhibits a structural phase transition at 510 K to a cubic high temperature form (HT) in which the Ni atoms form a FCC structure and the Mg atoms occupy the tetrahedral sites. In other words it is the same  $\text{CaF}_2$  structure we encountered for  $\text{YH}_2$  and  $\text{LaH}_2$ , Ni playing the role of Y or La and Mg playing the role of H. The low-temperature (LT) form of  $\text{Mg}_2\text{NiH}_4$  is seemingly much more complicated but is in fact a slightly distorted monoclinic  $\text{CaF}_2$  structure as shown in Fig. VII.4.

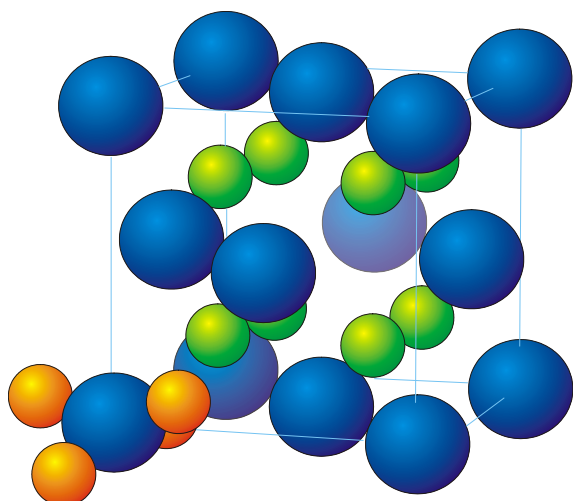
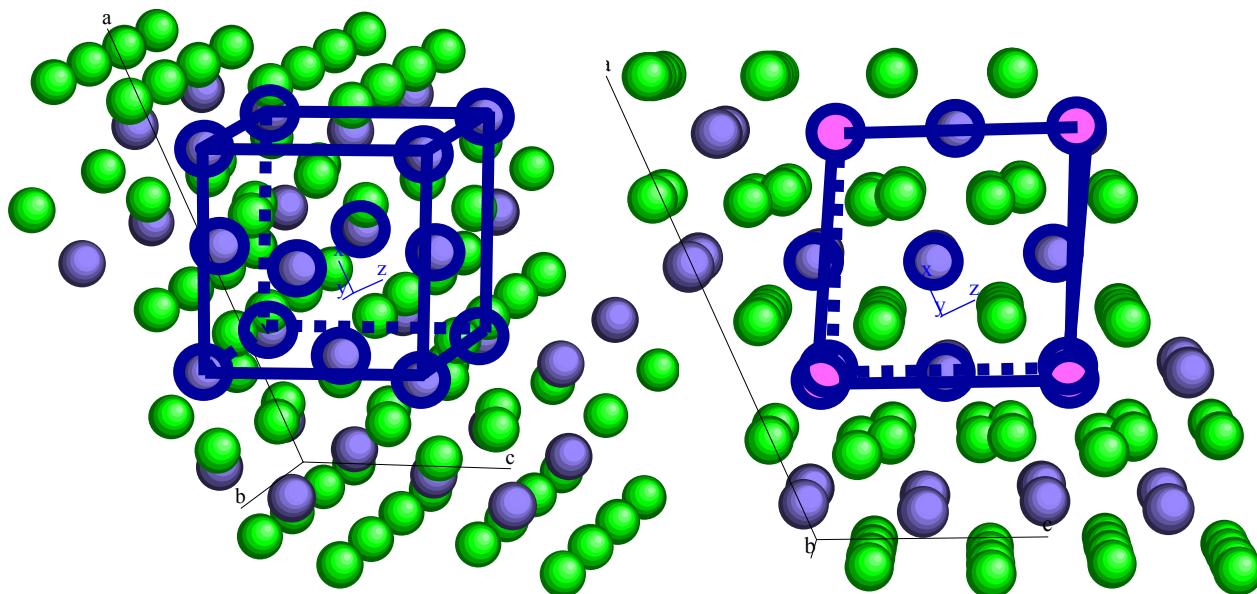
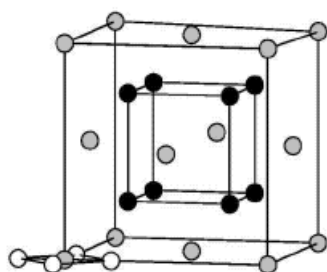
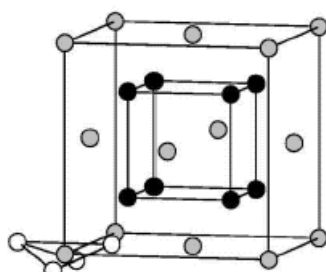


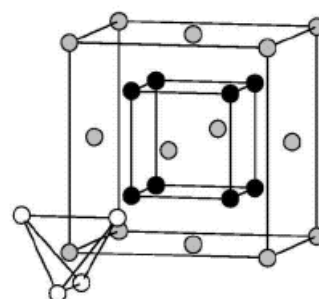
Fig. VII.4: Crystal structure of the high temperature phase (top two panels) and the low temperature phase of  $\text{Mg}_2\text{NiH}_4$ . The Ni atoms are in blue, the Mg atoms in green and the hydrogen atoms in orange. For clarity hydrogen is only shown near one Ni atom. The arrangement is that proposed by Garcia et al.<sup>17</sup> In the lower panel, we indicate three configurations that have been proposed for hydrogen in  $\text{Mg}_2\text{NiH}_4$ .



square planar



tetrahedrally deformed square planar



regular tetrahedral

Table VII.2: Structural parameters used by Garcia et al for the three hydrogen configurations in  $\text{Mg}_2\text{NiH}_4$  shown in Fig. VII.4. The lattice spacing is  $a$ . The values for  $x$  and  $z$  are given as fractions of  $a$ . The distances  $d$  refer to the nearest neighbour distances.

	Square planar	Tetrahedrally distorted square planar	Regular tetrahedral	Experimental
$a$ (Å)	6.507	6.507	6.507	6.507
$x$	0.2379	0.2208	0.1903	0.232
$z$	0.0	0.0883	0.1345	0.053
$d$ (Ni-Ni) (Å)	4.601	4.601	4.601	4.601
$d$ (Mg-Mg) (Å)	3.254	3.254	3.254	3.254
$d$ (Mg-Ni) (Å)	2.818	2.818	2.818	2.818
$d$ (Ni-H) (Å)	1.548	1.548	1.516	1.55
$d$ (Mg-H) (Å)	2.302	1.948	1.833	2.07
$d$ (H-H) (Å)	2.189	2.334	2.477	2.24
Bending angle ( $^\circ$ )	0.0	21.8	35.3	12.9

For the purpose of this lecture we shall only consider the cubic high temperature phase for which Garcia et al have calculated the band structure for the three hydrogen arrangements shown in the bottom panels of Fig. VII.4. As was the case for  $\text{YH}_3$  the exact position of hydrogen in  $\text{Mg}_2\text{NiH}_4$  was not easy to determine and there are still some uncertainties about the exact location of hydrogen. In spite of a considerable effort using neutron-diffraction techniques to determine the exact structure of the high-temperature phase the hydrogen distribution in the cubic HT of  $\text{Mg}_2\text{NiH}_4$  no final conclusion has been reached on the interpretation of these experimental data. This is the reason why in their recent theoretical article Garcia et al. calculated the band structure for various possibilities: a square arrangement of H around Ni, a tetrahedral arrangement and an intermediate arrangement, a tetrahedrally deformed square arrangement.

The most striking features of the corresponding structural data in Table VII.2 are the very large Ni-Ni separation and the short Ni-H bond. In metallic Ni that crystallizes in a FCC structure with  $a = 3.52$  Å,  $d$  (Ni-Ni) is 2.489 Å. For the band structure this implies that the d-band width is expected to be

$$\begin{aligned}
 W_d(\text{Ni in Mg}_2\text{NiH}_4) &= \left(\frac{2.489}{4.601}\right)^5 W_d(\text{Ni metal}) = \\
 &= 0.0463 \times W_d(\text{Ni metal}) \cong 0.3 \text{ eV}
 \end{aligned}
 \tag{VII.1}$$

since the d-d-overlap integrals are proportional to  $a^{-5}$ . This means that the d-band will be essentially flat. The short Ni-H distance is naively not expected since hydrogen is much more easily absorbed by Mg-metal than by Ni-metal. In  $\text{Mg}_2\text{NiH}_4$  one concludes that hydrogen prefer to form a  $(\text{NiH}_4)^{4-}$  complex that is then ionically bound to the  $\text{Mg}^{2+}$ -ions.

Our expectation of a very narrow d-band structure are confirmed by the band structure results shown in Fig. VII.5. These results show also that the nature of the ground state of  $\text{Mg}_2\text{NiH}_4$  depends crucially on the exact arrangement of the hydrogen atoms (in fact  $\text{H}^-$  ions) around the Ni-atoms. In their article Garcia et al. comment as follows: The hydrogen arrangement around the nickel atom has a noticeable impact on the band structure of the compound, mainly close to the Fermi level. As can clearly be seen from Fig. VII.5, the planar distribution is metallic, the regular tetrahedron semiconducting with an indirect gap, and the tetrahedrally distorted square-planar arrangement has a sort of pseudogap, i.e. a region around the Fermi level with a very low density of states. To understand these differences it is useful to have a general picture of the character of the bands of cubic  $\text{Mg}_2\text{NiH}_4$ . In the three cases shown in the figure, there is a separate set of four bands starting at around -10 eV. These are mainly hydrogen states corresponding to the four  $1s$  hydrogen orbitals. Between this group of bands and the Fermi level there are five bands corresponding mainly to the nickel  $3d$  orbitals. Above the Fermi level there is an empty magnesium  $3s$  band and a nickel  $4s$  band. As a result the magnesium is almost in a +2 state, transferring its two  $3s$  electrons to the  $(\text{NiH}_4)^{4-}$  complex. Four of the five  $3d$  nickel bands are almost flat and the upper one, whose main character is  $d_{x^2-y^2}$  is strongly dependent on

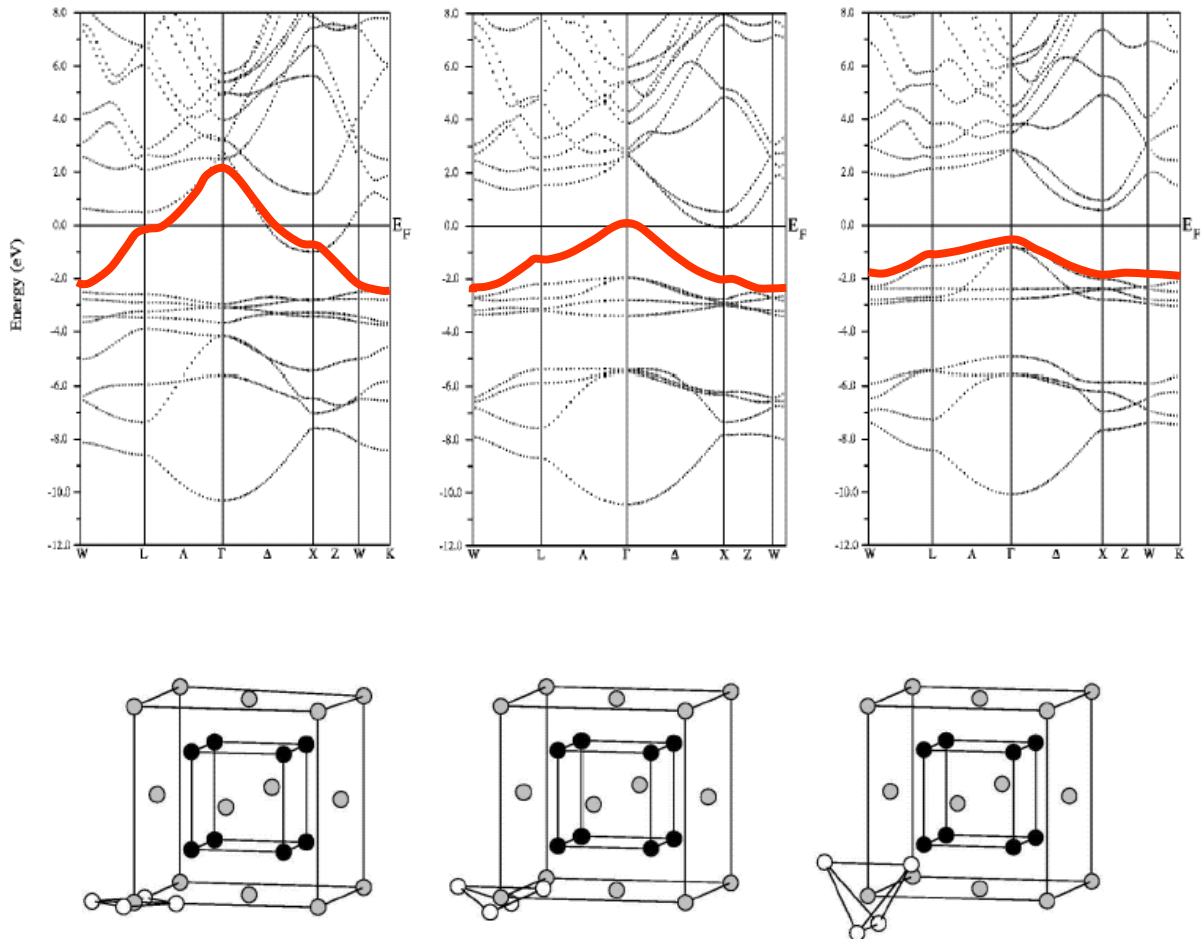


Fig. VII.5: Band structure calculations obtained by Garcia et al. for three different hydrogen arrangements in  $\text{Mg}_2\text{NiH}_4$ . The tetrahedrally deformed square planar arrangement is theoretically found to have the lowest total energy and is consistent with experimental data. Note that the optical gap is about 2 eV.

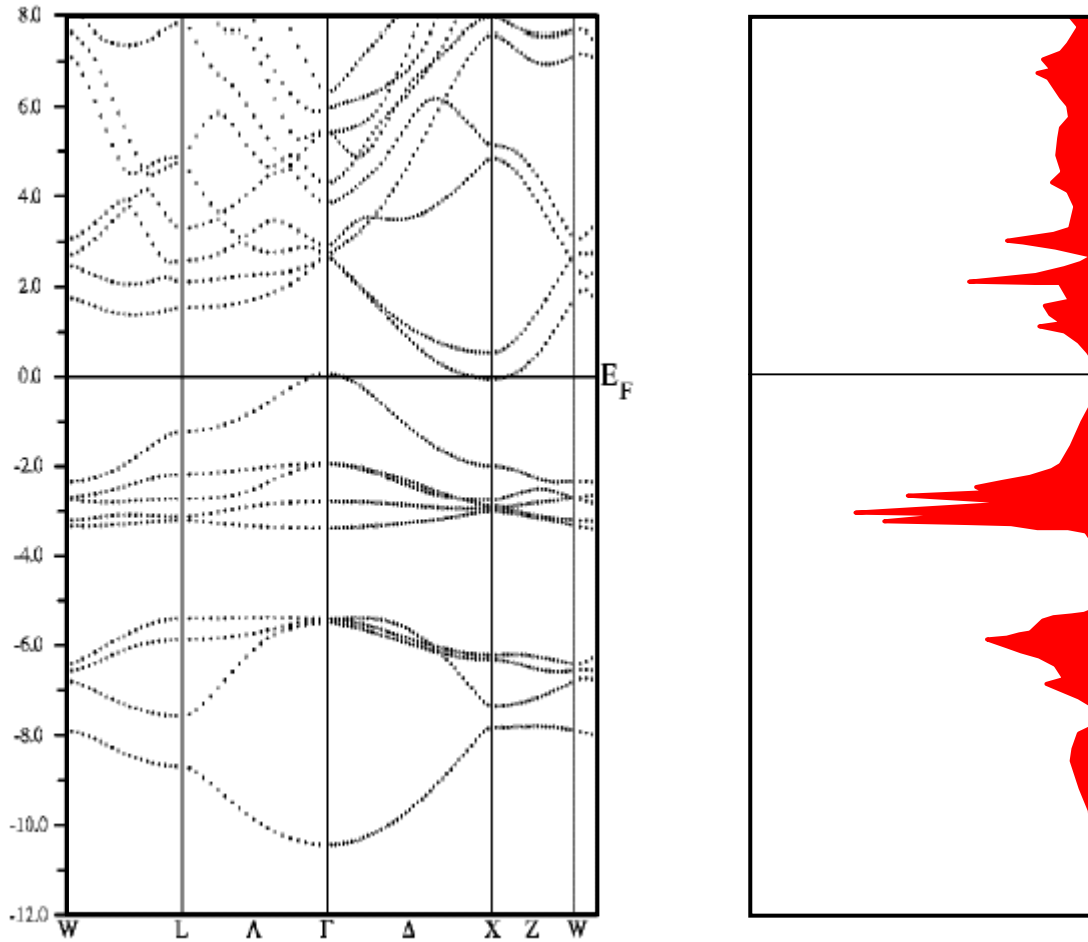


Fig. VII.6: The pseudogap (region of low density of states near the Fermi energy) of  $\text{Mg}_2\text{NiH}_4$  with the tetrahedrally deformed square planar arrangement of the hydrogen ions. The left panel shows the band structure and the left panel the corresponding density of states curve.

the hydrogen arrangement around the nickel atom. In the square-planar configuration this band is strongly hybridized with the hydrogen orbitals, mainly at the  $\Gamma$  point (center of the Brillouin zone). Because of this hybridization the energy is higher and the band crosses the Fermi level. Since the  $d_{x^2-y^2}$  orbital has its charge density mainly in the plane, by changing the bending angle the hybridization is reduced and the energy at the  $\Gamma$  point is lowered, thus opening a gap at some point. The minimum hybridization is obtained for the regular tetrahedral configuration where the band gap is a maximum. We demonstrate now that the characteristic features of the electronic structure of the three  $\text{Mg}_2\text{NiH}_4$  structures shown in Fig. VII.5 can be understood on the basis of a simple cluster model.

## VII.4 SQUARE PLANAR CLUSTER

We consider a cluster consisting of four hydrogen atoms on a planar square arrangement around a transition metal atom. The Schrödinger equation for one electron in this cluster is

$$\left[ -\frac{\hbar^2}{2m}\Delta + V_M(\mathbf{r}) + V_{H_1}(\mathbf{r}) + V_{H_2}(\mathbf{r}) + V_{H_3}(\mathbf{r}) + V_{H_4}(\mathbf{r}) \right] \Psi = E\Psi \quad (\text{VII.2})$$

In analogy with the dihydride problem considered in Chapter V we introduce the following notations for simplification

$$\bar{H}_i \equiv -\frac{\hbar^2}{2m}\Delta + V_i(\mathbf{r}) \quad (i = M, H_1, H_2, H_3, H_4) \quad (\text{VII.3})$$

where M stands for metal, and  $H_i$  for the hydrogen atoms on a square, respectively. The atomic wave functions are for the metal and the hydrogen atoms

$$|M_l\rangle \equiv \phi_l(\mathbf{M}-\mathbf{r}) \quad |H_j\rangle \equiv \phi_j(\mathbf{H}_j-\mathbf{r}) \quad (\text{VII.4})$$

with

$$\bar{H}_M|M_l\rangle \equiv \left[ -\frac{\hbar^2}{2m}\Delta + V_M(\mathbf{r}) \right] |M_l\rangle = E_{M_l}|M_l\rangle \quad (\text{VII.5})$$

$$\bar{H}_{H_j}|H_j\rangle \equiv \left[ -\frac{\hbar^2}{2m}\Delta + V_{H_j}(\mathbf{r}) \right] |H_j\rangle = E_{H_j}|H_j\rangle \quad (\text{VII.6})$$

where  $E_{M_l}$  and  $E_{H_j}$  are the energies of the electronic states of the metal atom and the hydrogen atom. Note, however, that here we need to consider the d-states of the metal as well as its s- and p- states. For a  $\text{NiH}_4$  cluster this means that we will have, in addition to the four hydrogen states, five 3d-states, one 4s-state and three 4p-states, i.e. 13 atomic states.

One could now seek a solution of the Schrödinger for one electron as a linear combination of the atomic states  $|M_l\rangle$  and  $|H_j\rangle$ , i.e.

$$\Psi = \sum_{l=1}^9 a_l |M_l\rangle + \sum_{j=1}^4 b_j |H_j\rangle \quad (\text{VII.7})$$

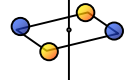
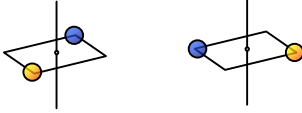
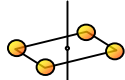
It is, however, more efficient to consider first the four hydrogen states separately. For these states the coefficient  $b_j$  are determined by the following matrix equation

$$\begin{pmatrix} E_H - 2V & -w & 0 & -w \\ -w & E_H - 2V & -w & 0 \\ 0 & -w & E_H - 2V & -w \\ -w & 0 & -w & E_H - 2V \end{pmatrix} \begin{pmatrix} b_1 \\ b_2 \\ b_3 \\ b_4 \end{pmatrix} = E \begin{pmatrix} b_1 \\ b_2 \\ b_3 \\ b_4 \end{pmatrix} \quad (\text{VII.8})$$

if only nearest neighbours on a square are considered. The eigenvalues are determined by the condition

$$\begin{vmatrix} E_H - 2V - E & -w & 0 & -w \\ -w & E_H - 2V - E & -w & 0 \\ 0 & -w & E_H - 2V - E & -w \\ -w & 0 & -w & E_H - 2V - E \end{vmatrix} = 0 \quad (\text{VII.9})$$

There are four energy eigenvalues (two are degenerate) and eigenvectors.

Eigenvalues	Eigenvectors	
$E = E_H - 2V + 2w$	$(1/2) (1, -1, 1, -1)$	
$E = E_H - 2V$	$(1/\sqrt{2}) (-1, 0, 1, 0)$ $(1/\sqrt{2}) (0, -1, 0, 1)$	
$E = E_H - 2V - 2w$	$(1/2) (1, 1, 1, 1)$	

The ground-state has s-symmetry, the two intermediate states p-symmetry and the highest energy state  $d_{x^2-y^2}$  symmetry. This means that in the  $13 \times 13$  matrix for the transition metal cluster with four hydrogen in a square planar arrangement most of the matrix elements vanish by symmetry. This is immediately evident from Fig. VII.7.

It is then straightforward to build up the matrix version of the Schrödinger equation. In order to have a non-trivial solution we have, as usual, to request that the corresponding  $13 \times 13$  determinant vanishes (see Fig. VII.8). To simplify the notation we have absorbed all the Coulomb-like terms (of the type  $-V$ ) in the new energies  $E_s$ ,  $E_p$ ,  $E_d$  and  $E_H$ . The overlap integrals are denoted by the letters  $t$ ,  $u$ ,  $v$ , and  $w$ . We see immediately that this problem reduces to a  $9 \times 9$  determinant since the  $p_z$ ,  $xy$ ,  $xz$  and  $yz$  states do not couple to any other states.

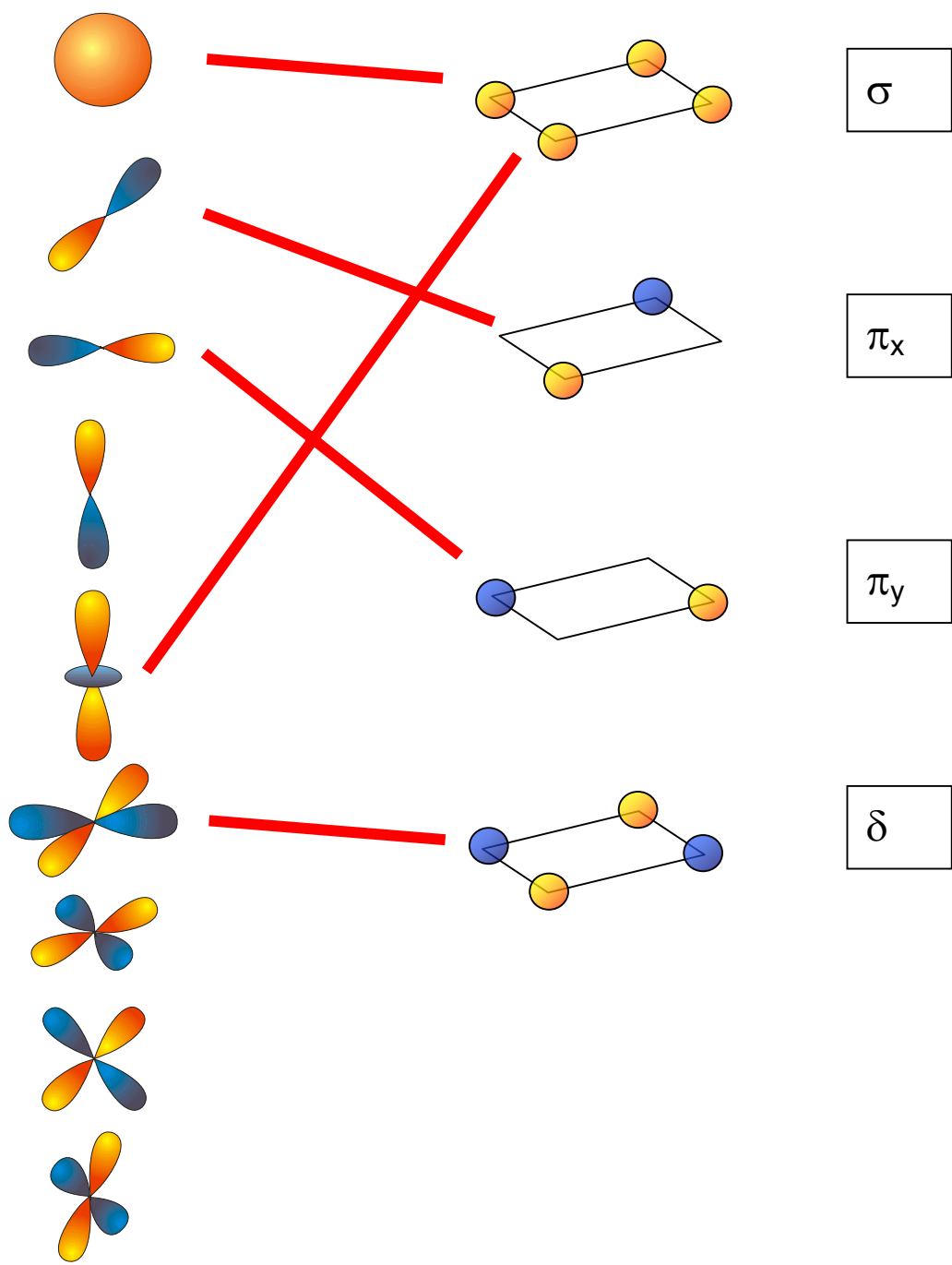


Fig. VII.7: The nine transition metal wave functions and the four symmetrized linear combinations of the four hydrogen atomic wave functions considered for the square planar cluster, e.g. for the NiH<sub>4</sub> cluster. The top linear combination has s-character, the two intermediate ones p-character (in fact p<sub>x</sub> and p<sub>y</sub>) and the bottom one has x<sup>2</sup>-y<sup>2</sup> character. The red lines indicate the combination of wave functions that have a non-vanishing overlap integral. The advantage to use symmetrized hydrogen wave functions is that only a small number of overlap integrals do not vanish.

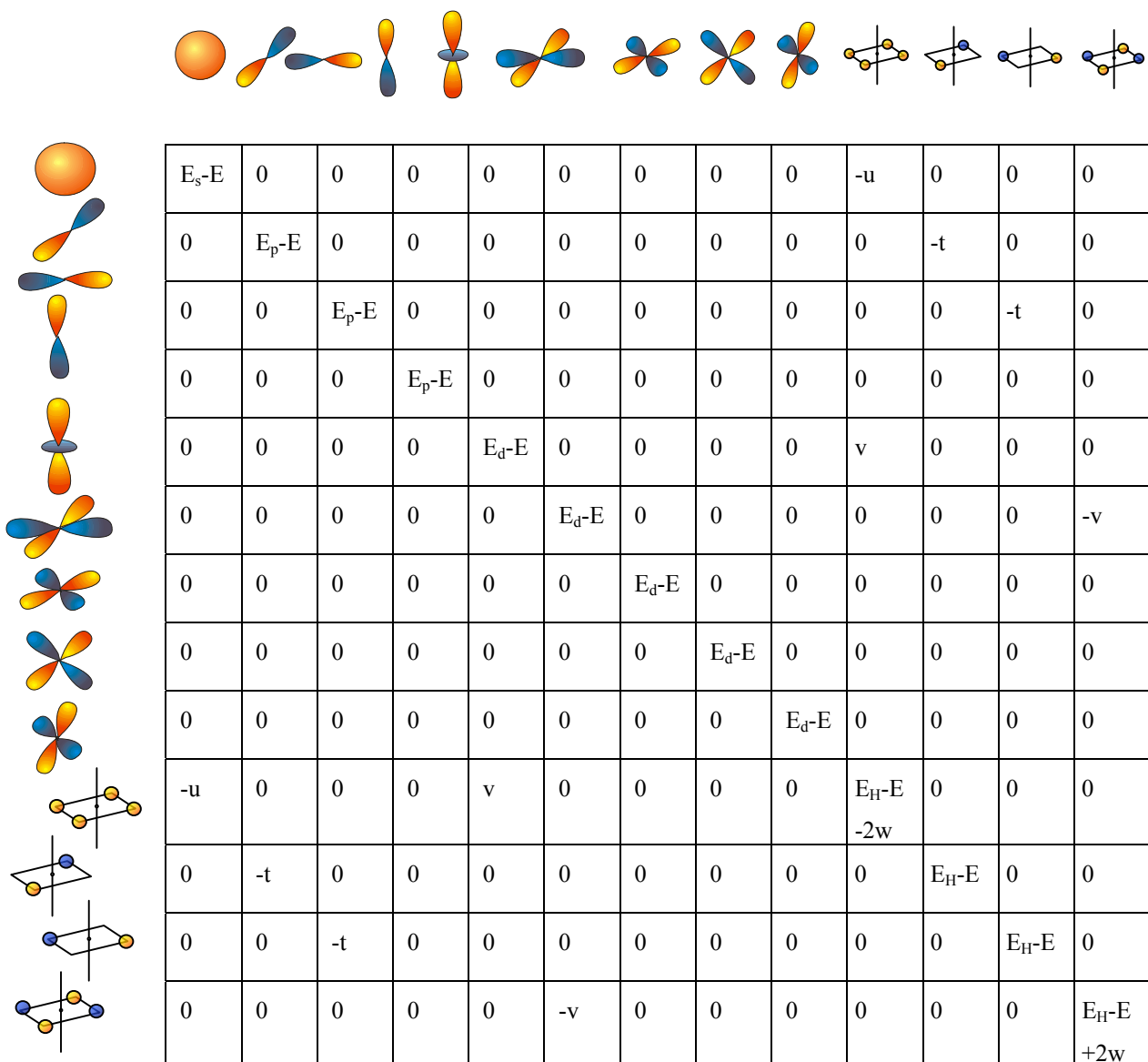


Fig. VII.8: Determinant for a cluster consisting of a transition metal and four hydrogen in a square planar arrangement.

As illustration we calculated the eigenvalues and eigenvectors corresponding to the following parameters  $E_s = -3$ ,  $E_p = 2$ ,  $E_d = -2$  and  $E_H = -4$  and  $t = 2$ ,  $u = 5$ ,  $v = 4$  and  $w = 1$ . These values are chosen so as to lead to level energies close to those of Garcia et al. (see Fig. VII.9). As expected from the form of the matrix the eigenvectors are linear combinations of two or at most three atomic states. The most important state is the antibonding state  $0.71(x^2 - y^2) - 0.71\delta$ . It is then easy to understand why moving hydrogen atoms out of the plane of the square leads to a lowering of

this state since the overlap is decreased. From this simple consideration one would expect a tetrahedral configuration since then the overlap between the  $(x^2-y^2)$  and  $\delta$  state is smallest. In this case the 18 electron rule follows directly from the fact that there is a large gap between the  $(x^2-y^2)$ - $\delta$  antibonding state and the next  $p_x - \pi_x$ ,  $p_y - \pi_y$  and  $p_z$  -states: the 10 Ni-, 4 Mg-, and 4 H- electrons can be accommodated in the lowest 9 levels (bands). To explicitly show how the cluster energy levels arise from the hybridisation of atomic levels, we indicate in Fig. VII.10 the

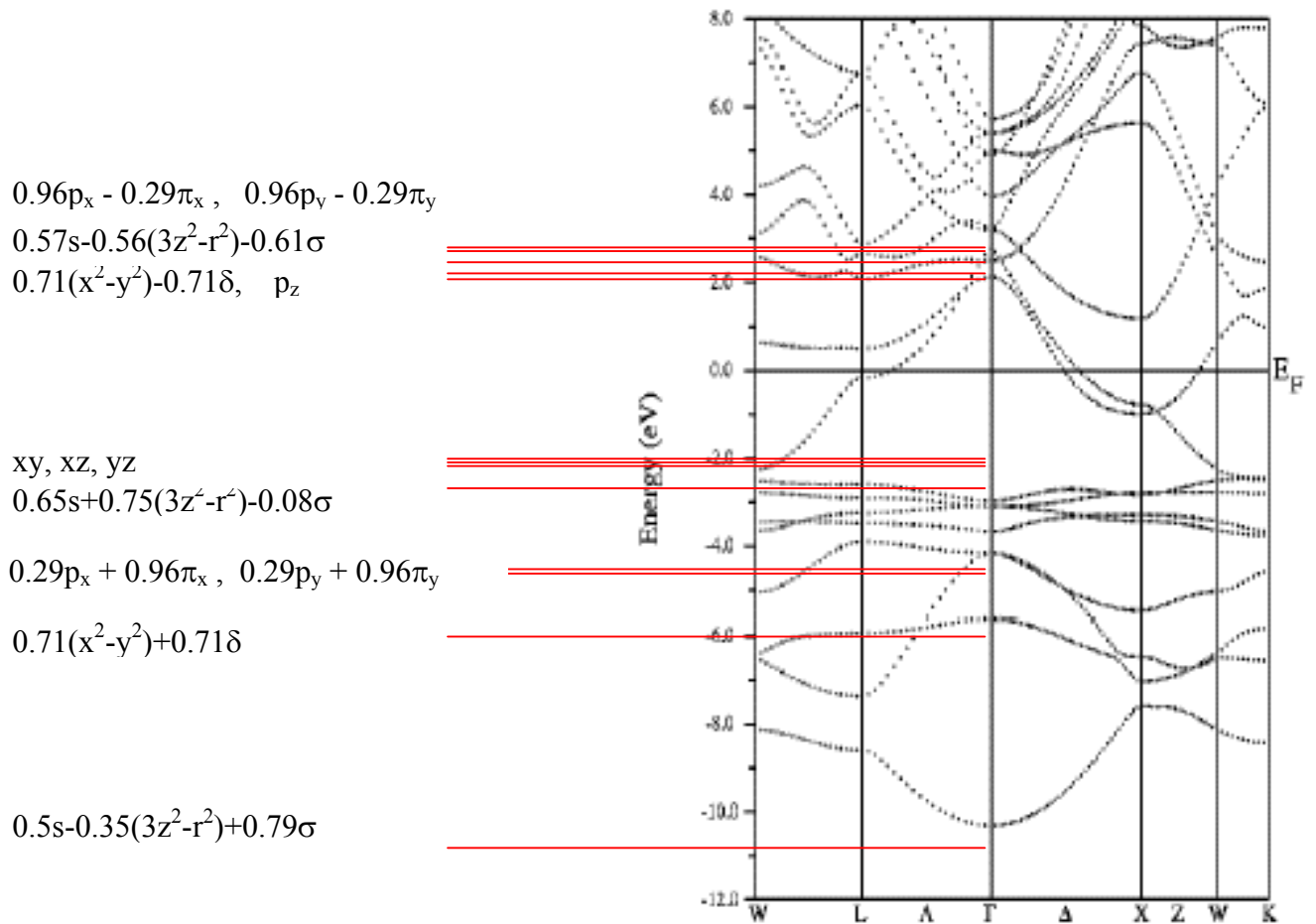


Fig. VII.9: Energy levels for a cluster consisting of a transition metal and four hydrogen in a square planar arrangement. For this numerical example we have chosen the following parameters  $E_s = -3$ ,  $E_p = 2$ ,  $E_d = -2$  and  $E_H = -4$  and  $t=2$ ,  $u=5$ ,  $v=4$  and  $w=2$ . The correspondence between the cluster levels and the energy band structure at the centre of the Brillouin zone is evident.

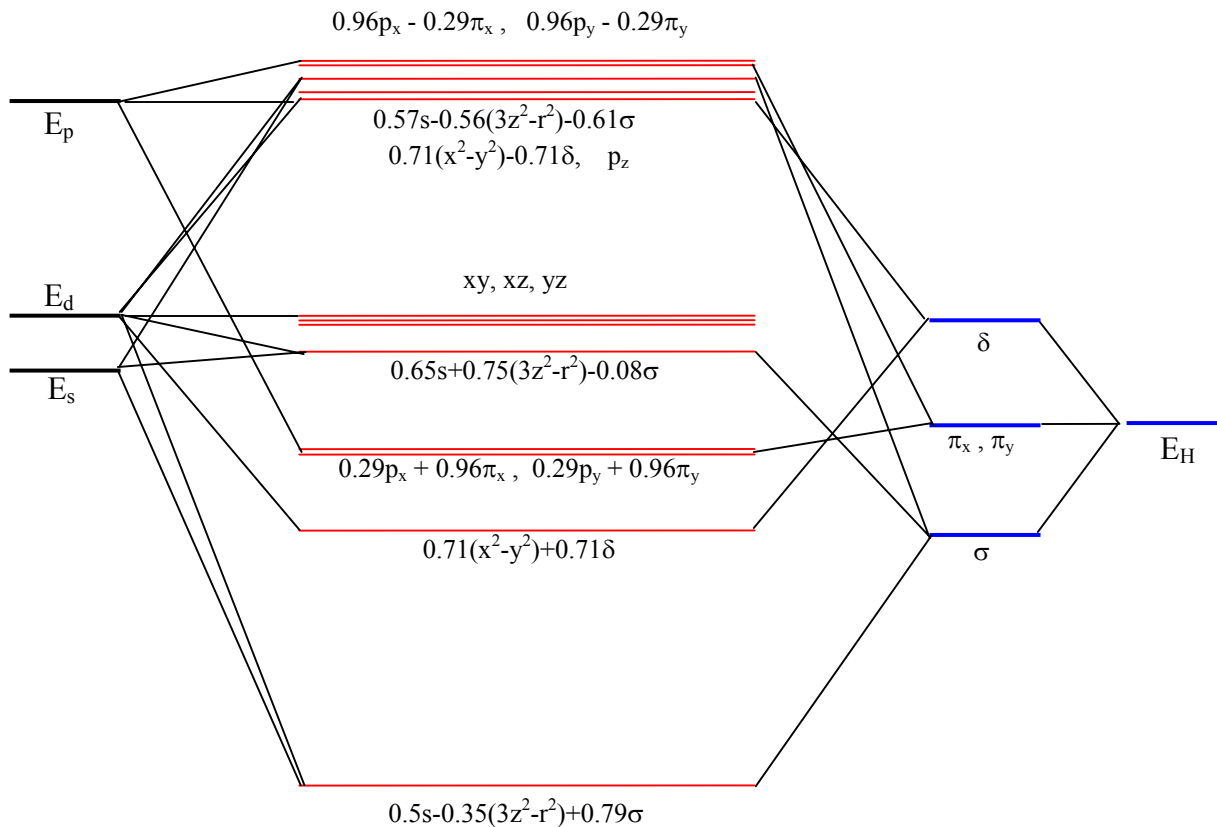


Fig. VII.10: Energy diagram corresponding to the cluster parameters chosen in Fig. VII.9. As expected from the form of the determinant in the eigenvectors corresponding to the various energy levels involve linear combination of at most 3 atomic levels.

energy diagram of the cluster considered in Fig. VII.9. Important for the understanding of the physics of  $Mg_2NiH_4$  is to realise that the energy gap depends essentially on the separation between energy levels determined by the complex cluster. In other words the Mg atoms do not seem to be important at all. This is explicitly shown by Garcia et al. in Fig. VII.11. The band structure in the right panel corresponds to a hypothetical solid in which the Mg atoms have been removed but without altering the position of the Ni and H atoms. The similarity between both band structures demonstrates that the physics of complex metal hydrides is essentially determined by the electronic structure of a single cluster.

Diagrams such as the one shown in Fig. VII.10 are very useful to indicate in a compact way the relation between the cluster energy levels and the original atomic levels. They can be generated for any complex geometry but it is not the purpose of this lecture to consider them all. We indicate only in the next subsection how one would proceed for an octahedral cluster and leave it as an exercise for the reader to treat for example the tetrahedral complex geometry.

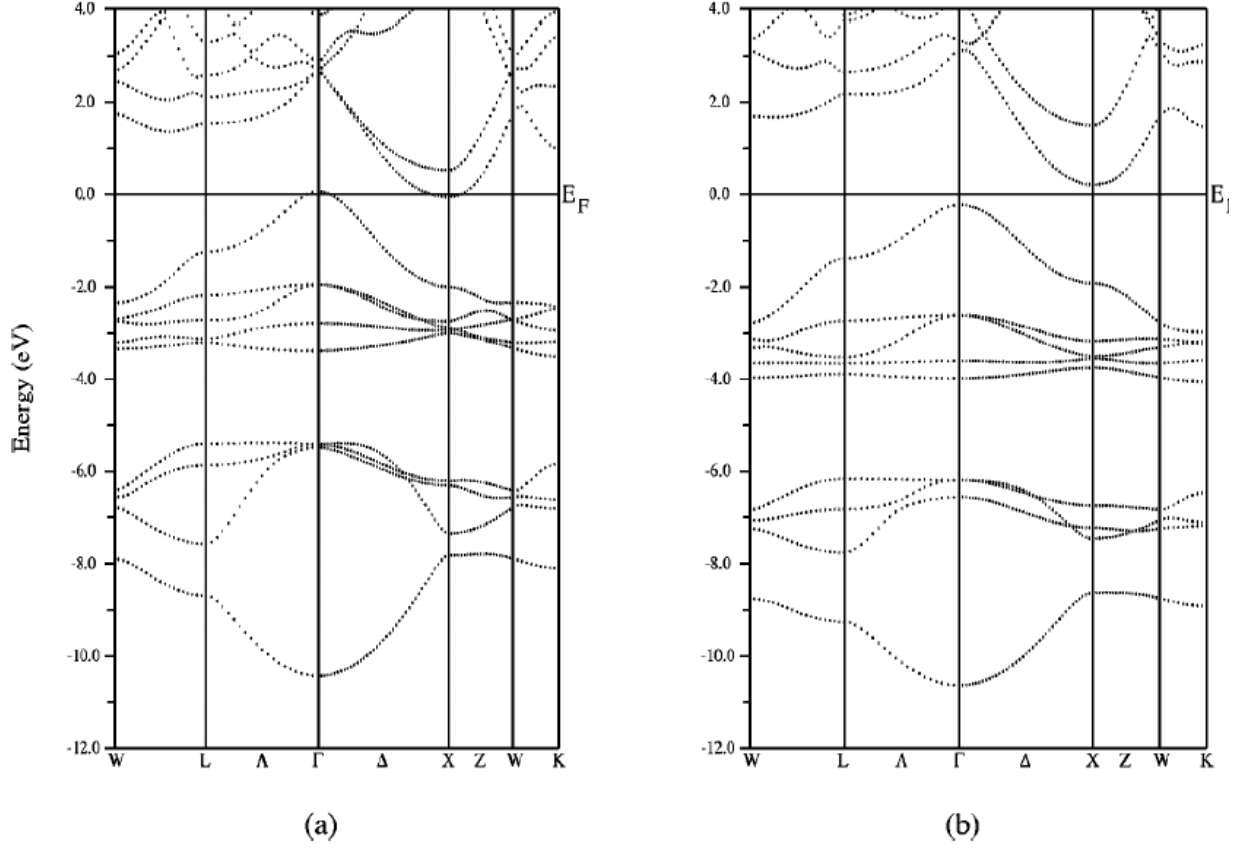


Fig. VII.11: Band structure of  $\text{Mg}_2\text{NiH}_4$  with hydrogen in a tetrahedrally deformed square arrangement (left panel). The band structure in the right panel corresponds to a hypothetical solid in which the Mg atoms have been removed but without altering the position of the Ni and H atoms. The similarity between both band structures demonstrate that the physics of complex metal hydrides is essentially determined by the electronic structure of a single cluster.

## VII.5 OCTAHEDRAL CLUSTER

We consider a cluster consisting of six hydrogen atoms forming a regular octahedron around a transition metal atom. The Schrödinger equation for one electron in this cluster is

$$\left[ -\frac{\hbar^2}{2m}\Delta + V_M(\mathbf{r}) + V_{H_1}(\mathbf{r}) + V_{H_2}(\mathbf{r}) + V_{H_3}(\mathbf{r}) + V_{H_4}(\mathbf{r}) + V_{H_5}(\mathbf{r}) + V_{H_6}(\mathbf{r}) \right] \Psi = E\Psi \quad (\text{VII.10})$$

and one seeks a solution as a linear combination of the atomic states  $|M_l\rangle$  and  $|H_j\rangle$ , i.e.

$$\Psi = \sum_{l=1}^9 a_l |M_l\rangle + \sum_{j=1}^6 b_j |H_j\rangle \quad (\text{VII.11})$$

Again it is more efficient to consider first the six hydrogen states separately.  
For these states the coefficient  $b_j$  are determined by the following matrix equation

$$\begin{pmatrix} E_H - 4V & -w & -w & -w & -w & 0 \\ -w & E_H - 4V & -w & 0 & -w & -w \\ -w & -w & E_H - 4V & -w & 0 & -w \\ -w & 0 & -w & E_H - 4V & -w & -w \\ -w & -w & 0 & -w & E_H - 4V & 0 \\ 0 & -w & -w & -w & -w & E_H - 4V \end{pmatrix} \begin{pmatrix} b_1 \\ b_2 \\ b_3 \\ b_4 \\ b_5 \\ b_6 \end{pmatrix} = E \begin{pmatrix} b_1 \\ b_2 \\ b_3 \\ b_4 \\ b_5 \\ b_6 \end{pmatrix} \quad (\text{VII.12})$$

if only nearest neighbours on the octahedron are considered. The eigenvalues are determined by the condition

$$\begin{vmatrix} E_H - 4V - E & -w & -w & -w & -w & 0 \\ -w & E_H - 4V - E & -w & 0 & -w & -w \\ -w & -w & E_H - 4V - E & -w & 0 & -w \\ -w & 0 & -w & E_H - 4V - E & -w & -w \\ -w & -w & 0 & -w & E_H - 4V - E & 0 \\ 0 & -w & -w & -w & -w & E_H - 4V - E \end{vmatrix} = 0 \quad (\text{VII.13})$$

There are six energy eigenvalues (two are degenerate) and eigenvectors.

Eigenvalues	Eigenvectors
$E = -4V + 2w$	$(1/2) (0, -1, 1, -1, 1, 0)$ $(1/\sqrt{12}) (1, -2, 1, -2, 1, 1)$
$E = -4V$	$(1/\sqrt{2}) (1, 0, 0, 0, 0, -1)$ $(1/\sqrt{2}) (0, 0, 1, 0, -1, 0)$ $(1/\sqrt{2}) (0, -1, 0, 1, 0, 0)$
$E = -4V - 4w$	$(1/\sqrt{6}) (1, 1, 1, 1, 1, 1)$

These six linear combinations are indicated in Fig. VII.12. It is then straightforward to write down the  $15 \times 15$  matrix.

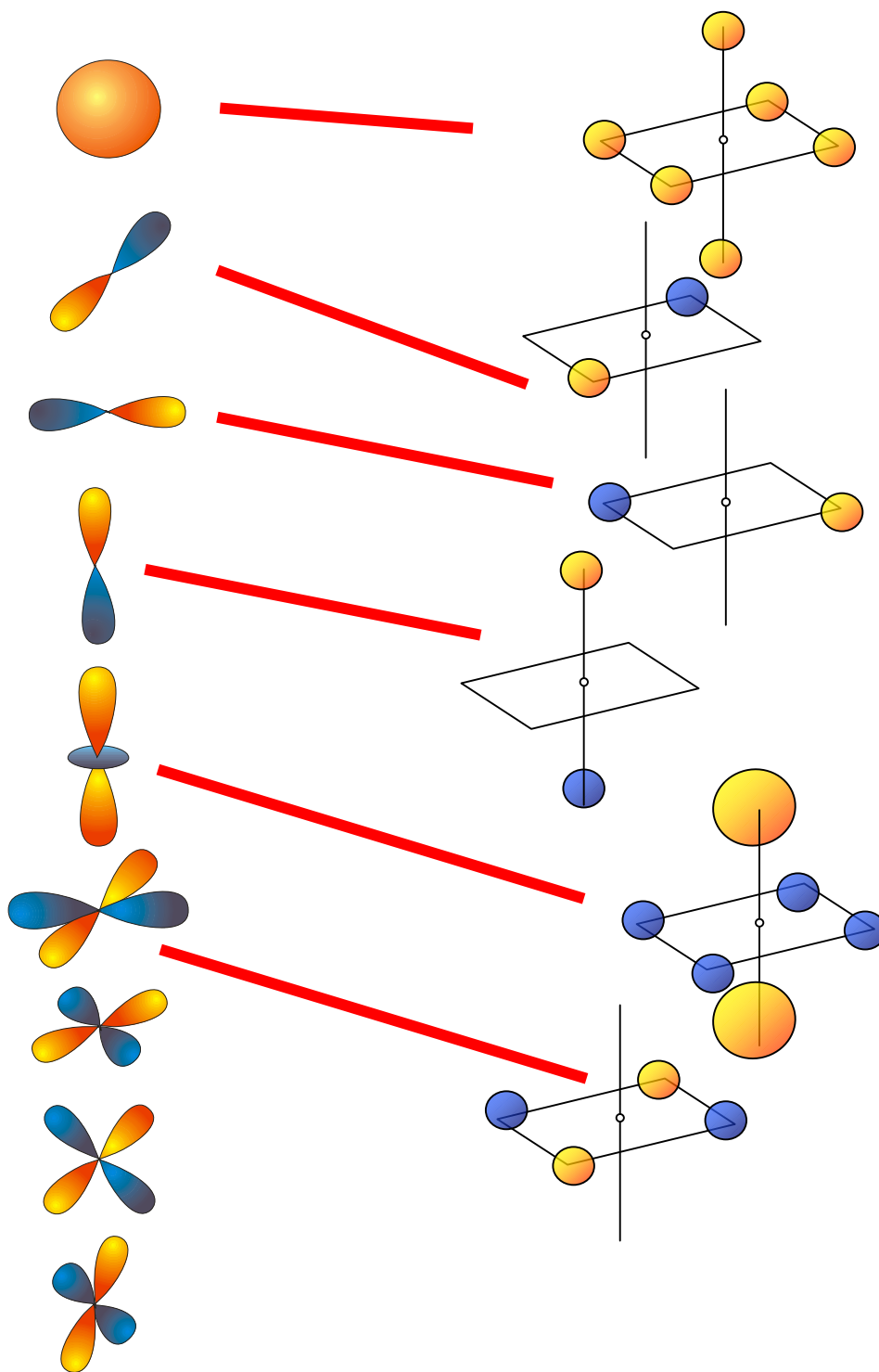


Fig. VII.12: The nine transition metal wave functions and the six symmetrized linear combinations of the six hydrogen atomic wave functions considered for the octahedron cluster, e.g. for the  $\text{NiH}_6$  cluster. The top linear combination has s-character, the three intermediate ones p-character (in fact  $p_x$ ,  $p_y$  and  $p_z$ ) and the bottom ones have  $3z^2 - r^2$  and  $x^2 - y^2$  character, respectively. The red lines indicate the combination of wave functions that have a non-vanishing overlap integral.

## VII.6 ALANATES

Complex hydrides of aluminum are attractive as hydrogen storage compounds due to their large hydrogen content. Unfortunately, their application in this manner has been impractical as a result of the great difficulties in reversing the hydrogen release reaction. Since workers in several laboratories have reported the discovery of a number of catalysts that improve the reversing of the hydrogen release by  $\text{NaAlH}_4$ ,  $\text{Na}_3\text{AlH}_6$ , and  $\text{LiAlH}_4$ , interest in the use of complex hydrides of aluminum as hydrogen storage media has been reactivated. Bogdanovicz and coworkers<sup>18</sup> have recently reported a study of the catalytic effects of transition metal compounds on both the hydrogen release and uptake by sodium aluminum hydrides. In this report, it was revealed that the chlorides of many transition metals improved the hydrogen release and also provided reversibility to those reactions. This work also includes the study of combinations of these transition metal compounds for use as catalysts. It was found that titanium and iron function synergistically in their catalytic effect, particularly so with titanium in the form,  $\text{Ti}(\text{OBu})_4$ . Jensen et al.<sup>19</sup> found that the catalytic effect of titanium in the form  $\text{Ti}(\text{OBu})_4$  depends on the method of its combination with the sodium aluminum hydride. These researchers reported

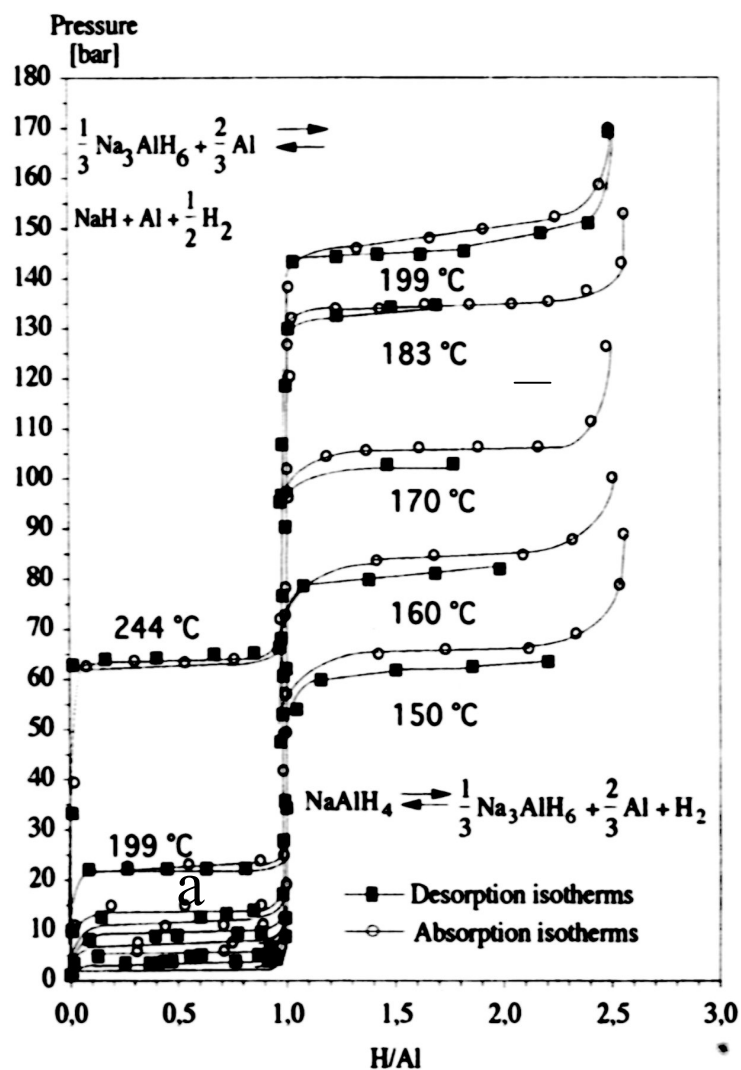


Fig. VII.13: Pressure-composition isotherms of  $\text{NaAlH}_4$

that mechanical introduction of the titanium compound to the sodium aluminum hydride produced far superior results to those obtained by Bogdanovicz using solution methods. Not only were there action rates increased for hydrogen uptake and release, the reversible hydrogen content was increased from the 3.2% reported by Bogdanovicz to 4.0%. This occurred by altering the first step of the dehydrogenation of NaAlH<sub>4</sub>, in which



In a second paper by Jensen and coworkers, it was reported that Zr(OPr)<sub>4</sub> also catalytically influenced the hydrogenation/dehydrogenation of sodium aluminum hydride. Mechanical incorporation of the catalyst into the hydride was again used, and it was found that this catalyst influenced the system differently than the titanium catalyst. While the titanium catalyst altered the first step of the decomposition of sodium aluminum hydride, the zirconium catalyst accelerated the second step,



It also was shown that titanium and zirconium can be incorporated simultaneously into a sample and function together to influence both steps in the dehydrogenation.

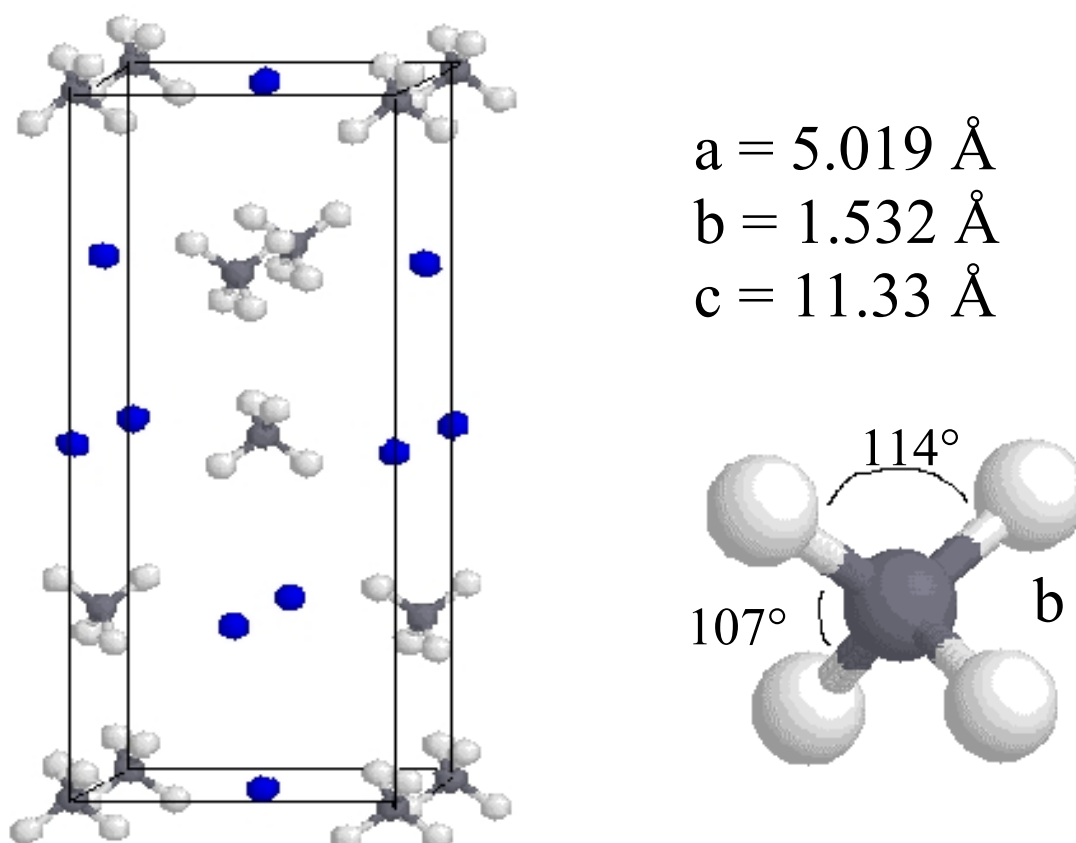


Fig. VII.14: Crystal structure of NaAlH<sub>4</sub>. The Na atoms are indicated in blue. A detail of the tetrahedral [AlH<sub>4</sub>]<sup>4-</sup> complex is shown on the right.

Zaluski and coworkers<sup>20</sup>, reported that lithium and sodium alanates could be prepared by ball milling. Three of the compounds produced in this work,  $\text{Na}_3\text{AlH}_6$ ,  $(\text{Li-Na})_3\text{AlH}_6$ , and  $(\text{Li-Na-B})_3\text{AlH}_6$ , were found to reversibly release hydrogen. These compounds absorbed and released hydrogen much more rapidly than the previously reported catalyzed systems.

The alanates are going to play a major role in the NWO program “Sustainable hydrogen”. One of the project is to explore thousands of compositions to discover the best possible compounds. The idea is to deposit a thin film of an alanate using various sources that are disposed in such a way that the film has a continuous variation of composition as a function of position. You may ask then how it will be possible to monitor hydrogen absorption in thousands of samples at the same time.. The answer to this question is a direct consequence of the band structure calculations made by Chou<sup>21</sup> and shown in Fig. VII.15. Similarly to the complex transition metal-hydrides there is a gap between the bands with strong hydrogen character and the Na-bands. The size of the gap implies that  $\text{NaAlH}_4$  is transparent. As it is expected that the existence of a gap is a general characteristic of alanates one can then detect the absorption of hydrogen in a sample optically. In a film with composition gradients it should therefore be straightforward to monitor simultaneously the absorption (and also its kinetics) of hydrogen in all parts of the sample. This is the great advantage of optical detection techniques.

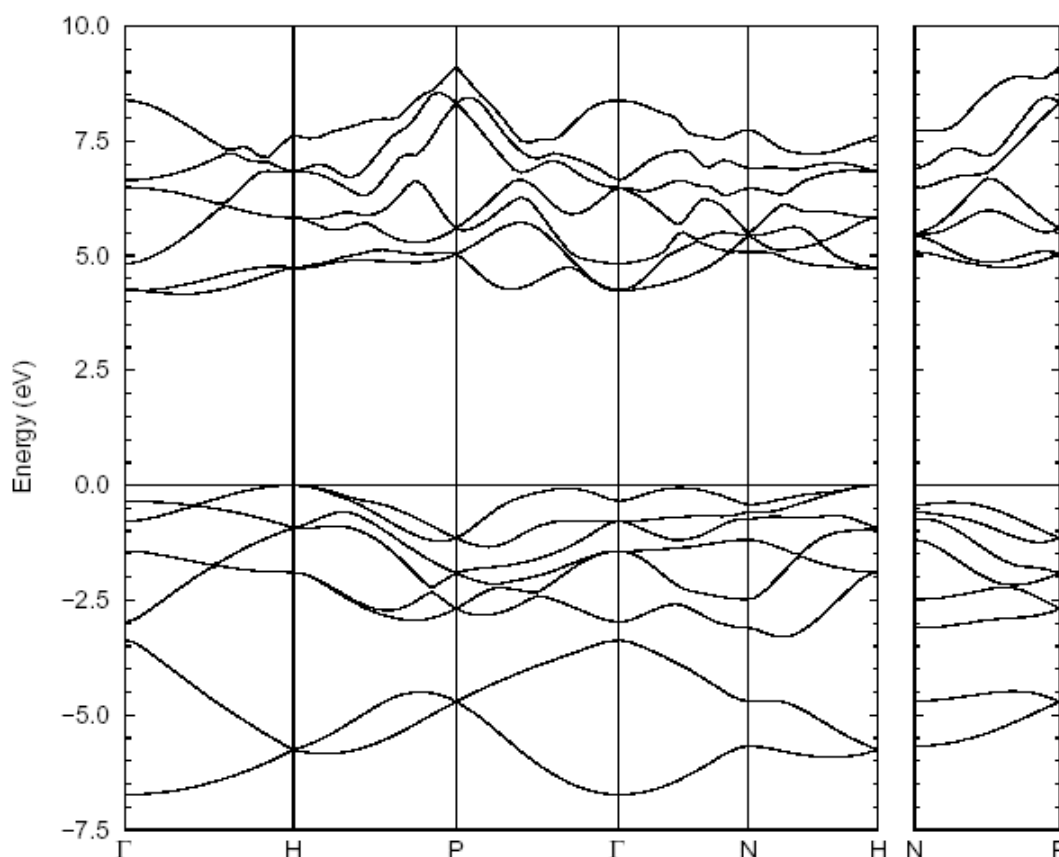


Fig. VII.15: Band structure of  $\text{NaAlH}_4$  as calculated by Chou<sup>21</sup>. Since there are two formula units per unit crystallographic cell the eight lowest bands are occupied. Remember that Na has 1 valence electron, Al: 3 and H: 1, i.e. 8 per formula unit.

## VII.7 ACKNOWLEDGEMENT

We are greatly indebted to K. Yvon for making available to us several essential papers on complex metal-hydrides.

## VII.8 REFERENCES

- <sup>1</sup> Sakai T., Natsuoka M. and Iwakura C., "Rare Earth Intermetallics for Metal-Hydrogen Batteries", Handbook on the Physics and Chemistry of Rare Earth **21** 135-180 (1995)
- <sup>2</sup> K. Yvon, in *Encycl. Inorg. Chem.*, John Wiley, Ed. R.B. King, **1994**, 3, 1401.
- <sup>3</sup> W. Bronger, *J. Alloys and Compounds*, **1995**, 229, 1.
- <sup>4</sup> M. Olofsson, K. Kadir, D. Noréus, *Inorg. Chem.* **1998**, 37, 2900, and references therein.
- <sup>5</sup> K. Yvon, *Chimia* 52 (1998) 613
- <sup>6</sup> N.T. Stetson, K. Yvon, P. Fischer, *Inorg. Chem.* **1994**, 33, 4598 ;
- <sup>7</sup> N.T. Stetson, K. Yvon, *J. Alloys and Compounds*, **1995**, 223, L4.
- <sup>8</sup> B. Huang, K. Yvon, P. Fischer, *J. Alloys and Compounds*, **1995**, 227, 121.
- <sup>9</sup> M. Bortz, B. Bertheville, K. Yvon, E.A. Movlaev, V.N. Verbetsky, F.Fauth, *J. Alloys and Compounds* **1998**
- <sup>10</sup> B. Huang, K. Yvon, P. Fischer, *J. Alloys and Compounds*, **1994**, 210, 243;
- <sup>11</sup> B. Huang, P. Fischer, K. Yvon, *J. Alloys and Compounds*, **1996**, 245, L24
- <sup>12</sup> B. Huang, K. Yvon, P. Fischer, *J. Alloys and Compounds*, **1995**, 227, 116.
- <sup>13</sup> B. Huang, K. Yvon, P. Fischer, *J. Alloys and Compounds*, **1994**, 204, L5.
- <sup>14</sup> M. Bortz, K. Yvon, P. Fischer, *J. Alloys and Compounds*, **1994**, 216, 39 and 43 ;
- <sup>15</sup> D.M. Heinekey, W.J. Oldham Jr., *Chem. Rev.* **1993**, 93, 913 ; R. Bau, M.H. Drabnis, *Inorg. Chim. Acta*, **1997**, 259, 25.
- <sup>16</sup> J.J. Reilly and R.H. Wiswall, *Inorg. Chem.* 7 (1968) 2254
- <sup>17</sup> G.N. Garcia, J.P. Abriata and J.O. Sofo, *Phys. Rev.* B59 (1999) 11746
- <sup>18</sup> B. Bogdanovicz, R. A. Brand, A. Marjanovic, M. Schwickardi, and J. Tolle, *J. Alloys and Compounds*, **302**, 36 (2000).
- <sup>19</sup> C. M. Jensen, R. Zidan, N. Mariels, A. Hee, and C. Hagen, *Int. J. Hydrogen E.*, **24**, 461 (1999).
- <sup>20</sup> L. Zaluski, A. Zaluska, and J.O. Ström-Olsen, *J Alloys and Compounds*, **290**, 71 (1999).
- <sup>21</sup> M.Y. Chou, private communication (2002)